Electrostatics on the sphere with applications to Monte Carlo simulations of two dimensional polar fluids.

Jean-Michel Caillol*

University of Paris-Sud, CNRS, LPT,

UMR 8627, Orsay, F-91405, France

(Dated: January 23, 2015)

Abstract

We present two methods for solving the electrostatics of point charges and multipoles on the surface of a sphere, *i.e.* in the space $\mathcal{S}_2$, with applications to numerical simulations of two-dimensional polar fluids.

In the first approach, point charges are associated with uniform neutralizing backgrounds to form neutral pseudo-charges, while, in the second, one instead considers bi-charges, *i.e.* dumbells of antipodal point charges of opposite signs. We establish the expressions of the electric potentials of pseudo- and bi-charges as isotropic solutions of the Laplace-Beltrami equation in $\mathcal{S}_2$. A multipolar expansion of pseudo- and bi-charge potentials leads to the electric potentials of mono- and bi-multipoles respectively. These potentials constitute non-isotropic solutions of the Laplace-Beltrami equation the general solution of which in spherical coordinates is recast under a new appealing form.

We then focus on the case of mono- and bi-dipoles and build the theory of dielectric media in $\mathcal{S}_2$. We notably obtain the expression of the static dielectric constant of a uniform isotropic polar fluid living in $\mathcal{S}_2$ in term of the polarization fluctuations of subdomains of $\mathcal{S}_2$. We also derive the long range behavior of the equilibrium pair correlation function under the assumption that it is governed by macroscopic electrostatics. These theoretical developments find their application in Monte Carlo simulations of the $2D$ fluid of dipolar hard spheres. Some preliminary numerical experiments are discussed with a special emphasis on finite size effects, a careful study of the thermodynamic limit, and a check of the theoretical predictions for the asymptotic behavior of the pair correlation function.

Keywords: Laplace-Beltrami equation on the sphere; Two-dimensional polar fluids; Monte Carlo simulations.

*Electronic address: Jean-Michel.Caillol@th.u-psud.fr

I. INTRODUCTION

The idea of using the two dimensional ($2D$) surface of a sphere, *i.e.* the space $\mathcal{S}_2$, to perform numerical simulations of a $2D$ fluid phase can be tracked back to a paper by J.-P. Hansen *et al.* devoted to a study of the electron gas at the surface of liquid Helium [1]. Subsequently, the same idea was used to study the crystallization of the $2D$ one-component plasma (with $\propto \log r$ interactions) [2], to establish the phase diagram of the $2D$ Coulomb gas [3], and to determine some thermodynamic and structural properties of the $2D$ polar fluid (with $\propto 1/r^2$ interactions) in its liquid phase [4, 5]. The generalizations to $3D$ systems, implying the use of the surface of a $4D$ hypersphere, *i.e.* the space $\mathcal{S}_3$, is due to Caillol and Levesque [6]. Some improvements on this early work, mostly applications concerning $3D$ polar fluids, were published recently [7].

Several simple ideas can be put forward to justify the use of a hyperspherical geometry in numerical simulations of plasmas and Coulombic fluids (*i.e.* fluids made of ions and/or dipoles) :

- (i) The n-dimensional non-Euclidian space $\mathcal{S}_n$ (in practice $n = 2, 3$), albeit finite, is homogeneous and isotropic, in the sense that it is invariant under the group $\mathcal{O}(n+1)$ of the $(n+1)D$ rotations of the Euclidian space E_{n+1}; it is thus well suited for the simulation of a fluid phase (in the bulk).

- (ii) The laws of electrostatics can easily be obtained in $\mathcal{S}_n$ and the Green's function of Laplace-Beltrami equation (*i.e.* Coulomb potential) is known [8]. It has a very simple analytical expression, tailor-made for numerical evaluations.

- (iii) The inclusion of charged or uncharged walls can easily be done in order to study the structure of liquids, plasmas, or colloïds at interfaces [6, 9–12]

The second point (ii) was partly overlooked by the authors of Ref. [4, 5] who used an empirical $2D$ dipole/dipole interaction, unfortunately *not* deduced from a solution of Laplace-Beltrami equation in $\mathcal{S}_2$, which casts some doubts on the validity of their results concerning the $2D$ Stockmayer fluid, notably those concerning its dielectric properties.

Some years after we are now in position to propose in this paper two possible, both rigorously correct, dipole/dipole pair-potentials and to use both of them into actual numerical simulations of a $2D$ dipolar hard sphere (DHS) fluid. Here, not only we extend to $\mathcal{S}_2$

the recent developments on $3D$ polar fluids in $\mathcal{S}_3$ discussed in Ref. [7], but we also present additional new results on multipolar expansions in $\mathcal{S}_2$, not yet available in $\mathcal{S}_3$, in Sec. II.

This article is thus a contribution to the physics of $2D$ fluids, colloïds or plasmas, the atoms or molecules of which interact *via* electrostatic pair potentials derived from a solution of the $2D$ Laplace equation. We emphasize that the systems that we consider cannot be seen as thin layers of real $3D$ systems. In this case, the electrostatic interactions should be derived from the solutions of the $3D$ Laplace equation. Simulations of such $3D$ systems constrained to live in a $2D$ geometry are nevertheless also possible in spherical geometries. In that case one should consider a $3D$ fluid of $\mathcal{S}_3$ made of particles interacting by pair potentials deduced from solutions of Laplace-Beltrami equation in $\mathcal{S}_3$ and constrained to stay on the equator of the hypersphere. This geometrical locus indeed identifies with the sphere $\mathcal{S}_2$. This approach was used for the $3D$ restricted primitive model of electrolytes in Ref. [13].

In this work our aim is to demonstate the validity of the sphere $\mathcal{S}_2$ to perform Monte Carlo (MC) simulations of a $2D$ polar fluid. We note that, although $2D$ dipolar fluids do not exist *per se* in nature, the model could be used via various mappings for applications as, recently, for the hydrodynamics of two-dimensional microfluids of droplets [14].

Our paper is organized as follows. After this introduction (Sec. I) we discuss in depth the electrostatics of the distributions of charges in $\mathcal{S}_2$ and their multipole expansions. The material reported in Sec. II is an intricate mixture of old and new stuff. The underlying idea is the remark of Landau and Lifchitz in Ref. [15] that, in a finite space such as $\mathcal{S}_2$, Laplace-Beltrami equation admits solutions if and only if the total electric charge of the space is equal to zero. Therefore, in $\mathcal{S}_2$, the building brick of electrostatics cannot be a single point charge q as in the ordinary $2D$ Euclidian space E_2. We are led instead to consider a pseudo-charge [6], a neologism denoting the association of a point charge and a uniform neutralizing background of opposite charge. Alternatively we can consider a bi-charge, *i.e.* a neutral dumbell made of two antipodal charges of opposite signs $+q$ and $-q$ as in Ref. [16]. Both approaches yield independent electrostatics theories which are sketched in Sec. II and III.

The case of dipoles is then examined more specifically in Sec. III. We need make a distinction between mono-dipoles, which are obtained as the leading term of a multipole expansion of a neutral set of pseudo-charges, and bi-dipoles, obtained in a similar way from bi-charges. As a consequence two possible microscopic models of dielectric media can be worked out, those made of mono-dipoles living on the entire sphere $\mathcal{S}_2$ and those made of

bi-dipoles living on the northern hemisphere $\mathcal{S}_2^+$.

These two types of models are then studied in the framework of Fulton's theory [17–20] in Sec. IV. Fulton's theory realizes a harmonious synthesis of linear response theory and the macroscopic theory of dielectric media. It allows us to obtain

- a family of formula for the dielectric constant ϵ of the fluid, well adapted for its determination in MC simulations.
- an expression for the asymptotic pair correlation in $\mathcal{S}_2$ under the assumption that it should be dictated by the laws of macroscopic electrostatics.

Monte-Carlo (MC) simulations of the $2D$ DHS fluid in the isotropic fluid phase are then discussed in Sec. V. We have chosen to report MC data only for two thermodynamic states, both in the isotropic fluid phase and extensive MC simulations of the $2D$ DHS fluid will be published elsewhere. These states could serve as benchmarks for future numeric studies. One of these states was studied many years ago in Ref. [21] by means of MC simulations within standard periodic boundary conditions (see also [22]). Comparisons of our results with those obtained in this pioneer work are OK. A carefull finite size scaling study of our data yields results of a high precision, notably for the energy, probably unattainable by standard simulation methods.

Conclusions are drawn in Sec (VI).

II. ELECTROSTATICS OF $2D$ CHARGES AND MULTIPOLES

A. The Plane

Let us first recall that the electrostatic potential $V_{E_2}(\boldsymbol{\rho})$ at a source-free point $\boldsymbol{\rho} = (x, y)$ of the Euclidian plane E_2 satisfies the 2D Laplace equation $\Delta_{\mathrm{E}_2} V_{E_2} = 0$, which in polar coordinates (ρ, φ) reads

$$\Delta_{\mathrm{E}_2} V_{E_2} = \frac{1}{\rho}\frac{\partial}{\partial \rho}\left(\rho \frac{\partial V}{\partial \rho}\right) + \frac{1}{\rho^2}\frac{\partial^2 V}{\partial \varphi^2} = 0 \ . \tag{1}$$

The general solution of Eq. (1) is [23, 24]

$$V_{E_2}(\rho, \varphi) = a_0 + b_0 \log \rho + \sum_{n=1}^{\infty} a_n \rho^n \cos(n\varphi + \alpha_n) + \sum_{n=1}^{\infty} b_n \rho^{-n} \cos(n\varphi + \beta_n) \ , \tag{2}$$

where a_n, b_n, α_n, and β_n are arbitrary constants. The terms of the *r.h.s.* of (2) which are singular at $\rho = 0$ may be interpreted as the potentials created by point multipoles located at the origin O, while those singular at $\rho = \infty$ as the potentials of point multipoles at infinity. In E_2 the potential of a point charge q located at O is $-q \log \rho$ up to an additional constant; it is the Green's function of Eq. (1) in E_2 (without boundaries) and it satisfies the 2D Poisson's equation

$$\Delta_{\mathrm{E}_2} \left(-\log \rho\right) = -2\pi \delta_{\mathrm{E}_2}(M, M_0) \equiv -2\pi \delta(x)\delta(y) \;, \tag{3}$$

where $\delta(x)$ denotes the 1D Dirac's distribution.

Finally, the Green's function $-\log(|\boldsymbol{\rho} - \boldsymbol{\rho}^{'}|)$ can be expanded in polar coordinates as [23]

$$-\log(|\boldsymbol{\rho} - \boldsymbol{\rho}^{'}|) = -\log \rho_< + \sum_{n=1}^{\infty} \frac{1}{n} \left(\frac{\rho_<}{\rho_>}\right)^n \cos\left(n\left(\varphi - \varphi^{'}\right)\right) \;, \tag{4}$$

where $\rho_< = \inf(\rho, \rho^{'})$ and $\rho_> = \sup(\rho, \rho^{'})$.

Eq. (4) serves as a starting point for the $2D$ multipolar expansion of Ref. [24]. Let us consider N charges q_i of polar coordinates (ρ_i, φ_i) and a point M (coordinates (ρ, φ)) of the plane E_2 such that $\rho > \rho_i$, $\forall i$. Making use of (4) one finds

$$\begin{aligned} V_{E_2}(M) &= -\sum_{i=1}^{N} q_i \log(|\boldsymbol{\rho} - \boldsymbol{\rho_i}|) \\ &= V_0 - \frac{1}{2}\sum_{\nu} Q_{0\nu} \log \rho + \frac{1}{2}\sum_{n=1}^{\infty}\sum_{\nu} \frac{1}{n\rho^n} Q_{n\nu} \exp(-in\nu\varphi) \;, \end{aligned} \tag{5}$$

where V_0 is some unessential constant. In (5) the index ν assumes the values -1 and $+1$ only. The complex multipolar moments are defined as

$$Q_{n\nu} = \sum_{i=1}^{N} q_i \rho_i^n \exp(in\nu\varphi_i) \;. \tag{6}$$

Since $Q_{n,-\nu} = Q^*_{n\nu}$ there are *at most* two independent multipole components at a given order n. The potential of a $2D$ multipole of order n therefore decays as $1/\rho^n$. This remark justifies *a posteriori* the interpretation that we gave for the terms of the *r.h.s.* of Eq. (2).

B. The Sphere

Here, we examine how the basic laws of $2D$ Euclidian electrostatics swiftly evoked in Sec. II A are changed when the system is wrapped on the surface of a sphere. Let us

first introduce some notations and recall some elementary mathematics. We denote by $\mathcal{S}_2(O,R)$ the sphere of center O and radius R of the usual 3D geometry. It is a (Riemannian) manifold of the $3D$ Euclidean space E_3 that we identify with $\mathbb{R}^3$. When we deal with the sphere of unit radius we adopt the uncluttered notation $\mathcal{S}_2 \equiv \mathcal{S}_2(O, R=1)$. Let M be the running point of $\mathcal{S}_2(O,R)$, we define the unit vector $\mathbf{z} \in \boldsymbol{\mathcal{S}_2}$ as $\boldsymbol{OM} = R\mathbf{z}$. The spherical coordinates are defined as usual : $\mathbf{z} = (\sin\theta\cos\varphi, \sin\theta\sin\varphi, \cos\theta)^T$ with $0 \leq \theta \leq \pi$ and $0 \leq \varphi < 2\pi$. The differential vector $d\mathbf{z} = d\theta\, \mathbf{e}_\theta + \sin\theta d\varphi\, \mathbf{e}_\varphi$ allows us to obtain two orthogonal unit vectors $(\mathbf{e}_\theta, \mathbf{e}_\varphi)$ that span the plane $\mathcal{T}_2(M)$ tangent to $\mathcal{S}_2(O,R)$ at point M. Recall that $\mathbf{e}_\theta = (\cos\theta\cos\varphi, \cos\theta\sin\varphi, -\sin\theta)^T$ and $\mathbf{e}_\varphi = (-\sin\varphi, \cos\varphi, 0)^T$. In addition and quite specifically since this notion cannot be generalized to higher dimensions, one has $\mathbf{e}_\varphi = \mathbf{z} \times \mathbf{e}_\theta$ where the symbol $\times$ denotes the $3D$ vectorial product. Finally the infinitesimal surface element is $dS = R^2 d\Omega$ where the infinitesimal solid angle $d\Omega = \sin\theta d\theta d\varphi$ in spherical coordinates.

In the sequel we will make a repeated use of the unit dyadic tensor $\mathbf{U}_{\mathcal{S}_2}(\mathbf{z}) = \mathbf{e}_\theta\mathbf{e}_\theta + \mathbf{e}_\varphi\mathbf{e}_\varphi$ of the plane $\mathcal{T}_2(M)$. Note that the unit dyadic tensor of Euclidian space E_3 is given by $\mathbf{U}_{E_3} = \mathbf{U}_{\mathcal{S}_2}(\mathbf{z}) + \mathbf{z}\mathbf{z}$. It is a constant tensor independent of point M. These admittedly old-fashioned objects however allow an easy definition of the gradient in $\mathcal{S}_2(O,R)$, or first differential Beltrami operator, as

$$\nabla_{\mathcal{S}_2(O,R)} = \mathbf{U}_{\mathcal{S}_2}(\mathbf{z}) \cdot \nabla_{E_3} \ ,$$

where ∇_{E_3} is the usual Euclidian gradient operator of E_3 and the dot in the r.h.s. denotes the 3D tensorial contraction. Note that, obviously, $\nabla_{\mathcal{S}_2(\mathrm{O,R})} = \nabla_{\mathcal{S}_2}/R$.

The Laplace-Beltrami operator (or second differential Beltrami operator) is defined in a similar way as the restriction of the $3D$ Euclidian Laplacian Δ_{E_3} to the surface of the sphere [25].

$$\Delta_{\mathcal{S}_2(0,\mathrm{R})} = \Delta_{E_3} - \frac{\partial^2}{\partial R^2} - \frac{2}{R}\frac{\partial}{\partial R} \ . \tag{7}$$

We have the scaling relation $\Delta_{\mathcal{S}_2(0,\mathrm{R})} \equiv \Delta_{\mathcal{S}_2}/R^2$ and, on the unit sphere, in spherical coordinates

$$\Delta_{\mathcal{S}_2} = \frac{1}{\sin\theta}\frac{\partial}{\partial\theta}\left(\sin\theta\frac{\partial}{\partial\theta}\right) + \frac{1}{\sin^2\theta}\frac{\partial^2}{\partial\varphi^2} \ . \tag{8}$$

$\Delta_{\mathcal{S}_2}$ identifies with minus the squared angular momentum operator of Quantum Mechanics; therefore it is a Hermitian operator the eigenvectors of which are the $3D$ spherical harmonics

$Y_l^m(\theta,\varphi)$ where l is a non-negative integer and the integer m satisfies $-l \leq m \leq +l$. Moreover $\Delta_{\mathcal{S}_2} Y_l^m = -l(l+1)Y_l^m$.

A general solution of Laplace-Beltrami equation in $\mathcal{S}_2$, *i.e.* $\Delta_{\mathcal{S}_2} V_{\mathcal{S}_2} = 0$, can easily be obtained in spherical coordinates by expanding $V_{\mathcal{S}_2}(\theta,\varphi)$ in Fourier series (see *e.g.* [26])

$$V_{\mathcal{S}_2}(\theta,\varphi) = \sum_{m=-\infty}^{m=+\infty} \hat{V}_m(\theta) e^{im\varphi} \ , \tag{9}$$

which yields for the Fourier coefficients

$$\sin\theta \frac{d}{d\theta} \sin\theta \frac{d}{d\theta} \hat{V}_m(\theta) = m^2 \hat{V}_m(\theta) \, . \tag{10}$$

In the above equation the change of variables $x = \log\tan\frac{\theta}{2}$ $(0 \leq \theta \leq \pi)$ leads to the elementary differential equation

$$\frac{d^2}{dx^2} \hat{V}_m(x) = m^2 \hat{V}_m(x) \ , \tag{11}$$

with the solutions

$$\hat{V}_0(x) \quad = a + bx \, , \ \text{for } m = 0 \ , \tag{12a}$$

$$\hat{V}_m(x) \ = K_{\pm m} e^{\pm m x} \ , \ \text{for } m \neq 0 \ , \tag{12b}$$

where a, b, and $K_{\pm m}$ are arbitrary complex constants. The general real solution of Laplace-Beltrami equation on the sphere can thus be finally written as

$$\begin{aligned} V_{\mathcal{S}_2}(\theta,\varphi) = a_0 + b_0 \log\tan\frac{\theta}{2} &+ \sum_{n=1}^{\infty} a_n \left[\tan\frac{\theta}{2}\right]^n \cos(n\varphi + \alpha_n) \\ &+ \sum_{n=1}^{\infty} b_n \left[\cot\frac{\theta}{2}\right]^n \cos(n\varphi + \beta_n) \ , \end{aligned} \tag{13}$$

where a_n, b_n, α_n, and β_n are arbitrary real constants. The terms of the *r.h.s.* of (13) which are singular at $\theta = 0$ may be interpreted as the potentials created by point multipoles located at the north pole $\mathcal{N}$ and those singular at $\theta = \pi$ as the potentials of point multipoles located at the south pole $\mathcal{S}$. Remarkably the isotropic term $\propto \log(\tan\theta/2)$ in the *r.h.s.* is singular both at $\theta = 0$ and $\theta = \pi$ and should identify with the potential of a unit bi-charge.

In order to check this assertion, let us first consider a bi-charge made of a charge $+q$ located at point M_0 of $\mathcal{S}_2(0,\mathrm{R})$ and its companion $-q$ located at the antipodal point $\overline{M}_0$ (with $\overline{\mathbf{z}}_0 = -\mathbf{z}_0$). The potential $V_{q,M_0}^{\mathrm{bi}}(M)$ at point M is the solution of Poisson's equation

$$\Delta_{\mathcal{S}_2} V_{q,M_0}^{\mathrm{bi}}(M) = -2\pi q \{ \delta_{\mathcal{S}_2}(\mathbf{z}_0,\mathbf{z}) - \delta_{\mathcal{S}_2}(\overline{\mathbf{z}}_0,\mathbf{z}) \} \ , \tag{14}$$

where the Dirac's distribution in $\mathcal{S}_2$ is defined as $\delta_{\mathcal{S}_2}(\mathbf{z}_0, \mathbf{z}) = \delta(1 - \mathbf{z}_0 \cdot \mathbf{z})$ [25]. Eq. (14) is solved by expanding both sides on spherical harmonics; after some elementary algebra one finds

$$\begin{aligned} V^{\mathrm{bi}}_{q,M_0}(M) &= q{\sum_l}' \frac{2l+1}{l(l+1)} P_l(\cos\psi_{M_0 M}) \\ &= -q - q\log\tan\frac{\psi_{M_0 M}}{2} , \end{aligned} \tag{15}$$

where $P_l(x)$ is a Legendre polynomial and the prime affixed to the sum in (15) means the restriction that l is an odd, positive integer. In this equation we have introduced the geodesic distance $\psi_{M_0 M} = \arccos(\mathbf{z}_0 \cdot \mathbf{z})$ between the two points M and M_0 on the unit sphere $\mathcal{S}_2$. The first term in the *r.h.s.* of Eq. (13) is thus indeed the potential created at a source-free point M by a point bi-charge located at the north pole $\mathcal{N}$.

It is the place to introduce Dirac's function on a sphere of radius $R \neq 1$; it will be denoted $\delta(M_0, M) = R^{-2}\delta_{\mathcal{S}_2}(\mathbf{z}_0, \mathbf{z})$. Since the Laplacian also scales as R^{-2} with the radius of the sphere the potential $V^{\mathrm{bi}}_{q,M_0}(M)$ is independent of the latter. Thus, in $\mathcal{S}_2(0, R)$, Poisson's equation for a bi-charge takes the form

$$\Delta_{\mathcal{S}_2(O,R)} V^{\mathrm{bi}}_{q,M_0}(M) = -2\pi q \left\{\delta(M_0, M) - \delta(\overline{M}_0, M)\right\} , \tag{16}$$

The electric field given by

$$\begin{aligned} \boldsymbol{E}^{\mathrm{bi}}_{q,M_0}(M) &= -\frac{1}{R}\nabla_{\mathcal{S}_2} V^{\mathrm{bi}}_{q,M_0}(M) \\ &= \frac{q}{R}\frac{1}{\sin\psi_{M_0 M}}\mathbf{t}_{M_0 M}(M) , \end{aligned} \tag{17}$$

where $\mathbf{t}_{M_0 M}(M) = \cot\psi_{M_0 M}\mathbf{z} - \mathbf{z}_0/\sin\psi_{M_0 M}$ denotes the unit vector, tangent to the geodesics $M_0 M$ at point M, and orientated from point M_0 towards point M [4, 5]. Note that this vector differs from $\mathbf{t}_{M_0 M}(M_0) = -\cot\psi_{M_0 M}\mathbf{z}_0 + \mathbf{z}/\sin\psi_{M_0 M}$ which is the unit vector, tangent to the geodesics $M_0 M$ at point M_0 (also orientated from M_0 to point M). One checks that the electric field $\boldsymbol{E}^{\mathrm{bi}}_{q,M_0}(M)$ satisfies to Gauss theorem [4, 5].

Let us consider now a *pseudo-charge* made of a point charge $+q$ located at at point M_0 of $\mathcal{S}_2$ and a uniform neutralizing background of charge density $-q/(4\pi)$. The potential $V^{\mathrm{ps}}_{q,M_0}(M)$ at point M is the solution of Poisson's equation

$$\Delta_{\mathcal{S}_2} V^{\mathrm{ps}}_{q,M_0}(M) = -2\pi q\{\delta_{\mathcal{S}_2}(\mathbf{z}_0, \mathbf{z}) - \frac{1}{4\pi}\} . \tag{18}$$

Eq. (18) can also be solved by expanding both sides on the complete basis set of spherical harmonics with the result

$$\begin{aligned} V^{\mathrm{ps}}_{q,M_0}(M) &= \frac{q}{2}\sum_{l=1}^{\infty}\frac{2l+1}{l(l+1)}P_l(\cos\psi_{M_0M}) \\ &= -\frac{q}{2} - q\log\sin\frac{\psi_{M_0M}}{2}\ , \end{aligned} \tag{19}$$

from which the electric field is readily obtained

$$\begin{aligned} \boldsymbol{E}^{\mathrm{ps}}_{q,M_0}(M) &= -\frac{1}{R}\nabla_{\mathcal{S}_2}V^{\mathrm{ps}}_{q,M_0}(M) \\ &= \frac{q}{2R}\cot\frac{\psi_{M_0M}}{2}\ \mathbf{t}_{M_0M}(M)\ , \end{aligned} \tag{20}$$

an expression which can also be obtained by applying Gauss theorem [4, 5]. Some remarks are in order.

- (i) One checks that, of course one has : $V^{\mathrm{bi}}_{q,M_0}(M) = V^{\mathrm{ps}}_{q,M_0}(M) - V^{\mathrm{ps}}_{q,\overline{M}_0}(M)$, since the backgrounds of the two pseudo-charges cancell each other.
- (i) For $R \neq 1$ one has

$$\Delta_{\mathcal{S}_2(O,R)}V^{\mathrm{ps}}_{q,M_0}(M) = -2\pi q\{\delta(M_0,M) - \frac{1}{S}\}\ . \tag{21}$$

  where $S = 4\pi R^2$ is the surface of $\mathcal{S}_2(0,R)$.
- (iii) Since the $3D$ distance between points M_0 and M, *i.e.* the length of the chord joining the two points is $d = 2R\sin(\psi_{M_0M}/2)$, it turns out that the expression of the potential of a pseudo-charge in $\mathcal{S}_2$ coincides with that of a point charge in the plane E_2.
- (iv) Although the potential of a pseudo-charge does not satisfies to Laplace-Beltrami equation at source-free points, the potentials created by neutral multipoles made of pseudo-charges indeed do, since the backgrounds cancell, as it will be seen below.

In order to extend the Green's function expansion (4) to the sphere we have found the following trick. Let us introduce, as in Ref. [27], the Cayley-Klein parameters

$$\alpha = \exp(i\varphi/2)\cos\frac{\theta}{2}\ , \tag{22a}$$

$$\beta = -i\exp(-i\varphi/2)\sin\frac{\theta}{2}\ . \tag{22b}$$

A short calculation reveals that, for two unit vectors $\mathbf{z}_1$ and $\mathbf{z}_2$ of $\mathcal{S}_2$, one has

$$|\alpha_1\beta_2 - \alpha_2\beta_1| = \sin\frac{\psi_{12}}{2} \ , \tag{23}$$

from which it follows that

$$\log\sin\frac{\psi_{12}}{2} = \log\sin\frac{\theta_>}{2} + \log\cos\frac{\theta_<}{2} + \log|1 - z\exp(i\Delta\varphi)| \ , \tag{24}$$

where $\theta_> = \sup(\theta_1, \theta_2)$, $\theta_< = \inf(\theta_1, \theta_2)$, $\Delta\varphi = \pm(\varphi_1 - \varphi_2)$, and $z = \tan(\theta_</2)/\tan(\theta_>/2)$. We note that $\log|1 - z\exp(i\Delta\varphi)| = (1/2)[\log(1 - z\exp(i\Delta\varphi)) + \log(1 - z\exp(-i\Delta\varphi))]$ and that, since $|z| < 1$, we can use the expansion of the complex logarithm $\log(1 - Z)$ within its circle of convergence, *i.e.* $\log(1 - Z) = -\sum_{n=1}^{\infty} Z^n/n$ for $|Z| < 1$, where $Z = z\exp(\pm i\Delta\varphi)$. In doing so, we obtain the following expansion :

$$\begin{aligned} -\log\sin\frac{\psi_{12}}{2} &= -\log\sin\frac{\theta_>}{2} - \log\cos\frac{\theta_<}{2} \\ &+ \sum_{n=1}^{\infty}\frac{1}{n}\left[\frac{\tan(\theta_</2)}{\tan(\theta_>/2)}\right]^n \cos(n\Delta\varphi) \ , \end{aligned} \tag{25}$$

which seems to be a new mathematical result. In order to make something usefull of that esthetic formula, we consider now a set of N pseudo-charges q_i of $\mathcal{S}_2(O, R)$, with spherical coordinates (θ_i, φ_i), and all around the north pole $\mathcal{N}$, *i.e.* $\pi \geq \theta_0 > \theta_i$, $\forall i = 1, \ldots, N$. A multipolar expansion of the electrostatic potential $V^{\mathrm{ps}}_{\mathcal{S}_2(O,R}(M)$ created by these charges at some point $M = (\theta, \varphi)$ of the surface of the sphere away from $\mathcal{N}$ follows from Eq. (25) under the assumption that $\pi \geq \theta \geq \theta_0$. One finds

$$\begin{aligned} V^{\mathrm{ps}}_{\mathcal{S}_2(O,R)}(M) &= -\sum_{i=1}^{N}\frac{q_i}{2} - \sum_{i=1}^{N} q_i \log\sin\frac{\psi_{M_iM}}{2} \\ &= V_0^{\mathrm{ps}} - \frac{1}{2}\sum_{\nu} Q_{0\nu}\log\left[2R\sin\frac{\theta}{2}\right] + \frac{1}{2}\sum_{n=1}^{\infty}\sum_{\nu}\frac{1}{nX^n}\, Q_{n\nu}\exp(-in\nu\varphi) \ , \end{aligned} \tag{26}$$

where V_0^{ps} is some unessential constant. In (26) the index ν assumes, as in Sec. II A, the values -1 and $+1$ only. On the sphere, the complex multipolar moments are defined as

$$Q_{n\nu} = \sum_{i=1}^{N} q_i X_i^n \exp(in\nu\varphi_i) \ . \tag{27}$$

In Eqs. (26) and (27) we have introduced the variables $X = 2R\tan(\theta/2)$ not to be confused with the length $2R\sin(\theta/2)$ of the chord $\overset{\frown}{NM}$ which constitutes the argument of the "log" term in the *r.h.s.* of (26).

We note that, since $Q_{n,-\nu} = Q^*_{n\nu}$, there are two independent multipoles of order n only (except for the charge of the distribution, *i.e.* the degenerate case $n = 0$). In the thermodynamic limit $\rho = R\theta$ fixed, $R \to \infty$ we have $X \to \rho$ and the multipole moments (27) as well as the multipolar expansion of the potential in (26) reduces to their "Euclidian" expressions in the plane $\mathcal{T}(\mathcal{N})$ tangent to the sphere at the north pole $\mathcal{N}$, resp. Eqs. (6) and (5). We remark that quite generally a point multipole located at some point M of $\mathcal{S}_2$ coincides with a $2D$ Euclidian point multipole in the tangent plane $\mathcal{T}(M)$ with the same complex moments $Q_{n\nu}$. Therefore the electrostatic potential $Q_{n\nu}\exp(-in\nu\varphi)/(nX^n)$ in the *r.h.s.* of (26) may be interpreted as the potential created by a multipole of order n and value $Q_{n\nu}$ located at the north pole $\mathcal{N}$ of the sphere. If $n \neq 0$ it clearly is a non-isotropic solutions of Laplace-Beltrami equation, singular at $\theta = 0$, *cf* Eq. (13).

For the sake of completeness we consider now a set of N bi-charges of $\mathcal{S}_2(O,R)$. Let q_i ($i = 1, \ldots, N$) be the point charges located in the northern hemisphere at the points M_i with spherical coordinates (θ_i, φ_i). Their N companions $-q_i$ are located at the antipodal points $\overline{M}_i$ in the southern-hemisphere, with coordinates $\overline{\theta}_i = \pi - \theta_i$ and $\overline{\varphi}_i = \pi + \varphi_i$. We will denote by $V^{\rm bi}_{\mathcal{S}_2(O,R)}(M)$ the electrostatic potential at some point M of the surface of the sphere. Assuming that $\theta_i < \theta < \pi - \theta_i$, $\forall i$ and making use of (25) one finds

$$
\begin{aligned}
V^{\rm bi}_{\mathcal{S}_2(O,R)}(M) &= V^{\rm ps}_{\mathcal{S}_2(O,R)}(M) + \sum_{i=1}^{N} \frac{q_i}{2} + \sum_{i=1}^{N} q_i \log\sin(\frac{\psi_{\overline{M}_i M}}{2}) \ , \\
&= V_0^{\rm bi} - \frac{1}{2}\sum_{\nu} Q_{0\nu} \log\left[2R\tan\frac{\theta}{2}\right] + \\
&+ \frac{1}{2}\sum_{n=1}^{\infty}\sum_{\nu} \frac{Q_{n\nu}\exp(-in\nu\varphi)}{n[2R]^n}\left\{\left[\cot\frac{\theta}{2}\right]^n - (-1)^n\left[\tan\frac{\theta}{2}\right]^n\right\} \ , \qquad (28)
\end{aligned}
$$

where $V_0^{\rm bi}$ is some irrelevant constant. The complex multipole moment $Q_{n\nu}$ has been defined in Eq. (27). The contribution $n = 0$ is the potential of a point bi-charge of total charge $\sum_i q_i$ and located at the north pole $\mathcal{N}$. The contribution $n \neq 0$ is that of a point multipole of order n and complex moment $Q_{n\nu}$ located at $\mathcal{N}$ (and its dumbell companion at the south pole $\mathcal{S}$). Its electrostatic potential has two singularities in $\theta = 0$ and $\theta = \pi$ (as expected) and it is one of the non-isotropic solution of Laplace-Beltrami Eq. (13). To distinguish the two types of multipoles encountered in this section, we shall christen mono-multipoles those obtained from pseudo-charges and bi-multipoles those obtained from bi-charges.

III. DIPOLES

A. The electric potential of a point dipole

Henceforth we specialize in the case of dipoles. We start with a point mono-dipole located at the north pole $\mathcal{N}$. It may be seen as a system of $N = 2$ pseudo-charges of $\mathcal{S}_2(O, R)$: a first charge δq with spherical coordinates $(\delta\theta_0, \varphi_0)$ and a second one with opposite sign $-\delta q$ and coordinates $(\delta\theta_0, \varphi_0 + \pi)$. We then take the limit $\delta q \to \infty$ and $\delta\theta_0 \to 0$ with the constraint that the *dipole moment* $\mu = 2R\theta_0\delta q$ is fixed. In this limit the vectorial moment $\boldsymbol{\mu} = \mu\,(\cos\varphi_0\,\mathbf{e}_x + \sin\varphi_0\,\mathbf{e}_y)$ belongs to the horizontal plane $\mathcal{T}(\mathcal{N}) \equiv (\mathbf{e}_x, \mathbf{e}_y)$ and its two non-zero complex multipole moments are $Q_{n\nu} = \delta_{1,n}\mu\exp(i\nu\varphi_0)$ where $\nu = \pm 1$. By inserting this expression in Eq. (26) one obtains the dipolar potential at some point M of the sphere

$$V^{\text{mono}}_{\mathcal{N},\boldsymbol{\mu}}(M) = \frac{\mu}{2R}\cos(\varphi - \varphi_0)\cot\frac{\theta}{2}\,. \tag{29}$$

In a similar way, one obtains for a bi-dipole located at the north pole $\mathcal{N}$

$$V^{\text{bi}}_{\mathcal{N},\boldsymbol{\mu}}(M) = \frac{\mu}{2R}\cos(\varphi - \varphi_0)\left\{\cot\frac{\theta}{2} + \tan\frac{\theta}{2}\right\}\,. \tag{30}$$

Note that $V^{\text{mono}}_{\mathcal{N},\boldsymbol{\mu}}(M)$ is a solution of Laplace-Beltrami Eq. (13) since the backgrounds of the two charges $\pm\delta q$ cancell each other. There is a single singularity in $\theta = 0$. In the thermodynamic limit $R \to \infty$, $\rho = R\theta$ fixed one recover the Euclidian dipolar potential $\boldsymbol{\mu}\cdot\boldsymbol{\rho}/\rho^2$ of a $2D$ dipole of the $(\mathbf{e}_x, \mathbf{e}_y)$ plane. $V^{\text{bi}}_{\mathcal{N},\boldsymbol{\mu}}(M)$ is also a solution of Laplace-Beltrami Eq. (13) but with two singularities at $\theta = 0$ and $\theta = \pi$. Note that the dipoles at the south-pole and the north-pole are the same vectors of E_3. The additional term $\tan(\theta/2)$ in the potential vanishes in the thermodynamic limit $R \to \infty$, $\rho = R\theta$ fixed, and does not change the conclusion that one also recovers the Euclidian dipolar potential in this limit for the bi-dipole.

In the general case where the dipole say $\boldsymbol{\mu}_0$ of modulus $\mu = \|\boldsymbol{\mu}_0\|$ is located at some point

M_0 of $\mathcal{S}_2(O,R)$ one obviously have

$$V^{\text{mono}}_{M_0,\boldsymbol{\mu}_0}(M) = \frac{\mu}{2R}\,\cot\frac{\psi_{M_0M}}{2}\,\mathbf{s}_0\cdot\mathbf{t}_{MM_0}(M_0)$$
$$= \frac{\mu}{4R}\frac{1}{\sin^2\frac{\psi_{M_0M}}{2}}\,\mathbf{s}_0\cdot\mathbf{z} \tag{31a}$$
$$V^{\text{bi}}_{M_0,\boldsymbol{\mu}_0}(M) = V^{\text{mono}}_{M_0,\boldsymbol{\mu}_0}(M) + V^{\text{mono}}_{\overline{M}_0,\boldsymbol{\mu}_0}(M) \tag{31b}$$
$$= \frac{\mu}{R}\,\frac{1}{\sin\psi_{M_0M}}\,\mathbf{s}_0\cdot\mathbf{t}_{MM_0}(M_0)$$
$$= \frac{\mu}{R}\frac{1}{\sin^2\psi_{M_0M}}\,\mathbf{s}_0\cdot\mathbf{z}\ , \tag{31c}$$

where we have introduced the unit vector $\mathbf{s}_0 = \boldsymbol{\mu_0}/\mu$.

B. The electric field of a point dipole

The electric field created by a mono-dipole located at some point M_0 is obtained by taking minus the gradient of the potential $V^{\text{mono}}_{M_0,\boldsymbol{\mu}_0}(M)$ at point M with the result :

$$\mathbf{E}^{\text{mono}}_{M_0,\boldsymbol{\mu}_0}(M) = -\frac{1}{R}\cdot\nabla_{\mathcal{S}_3,M}V^{\text{mono}}_{M_0,\boldsymbol{\mu}_0}(M) = 2\pi\mathbf{G}^{\text{mono}}_0(M,M_0)\cdot\boldsymbol{\mu}_0\ , \tag{32}$$

where we have introduced, as in Ref. [7], the tensorial dipolar Green's function $\mathbf{G}^{\text{mono}}_0(M,M_0)$, for which we give two useful expressions :

$$\mathbf{G}^{\text{mono}}_0(M,M_0) = \frac{1}{4\pi R^2}\frac{1}{1-\cos\psi_{M_0M}}$$
$$\left[(1+\cos\psi_{M_0M})\,\mathbf{t}_{MM_0}(M)\mathbf{t}_{MM_0}(M_0) - \mathbf{U}_{\mathcal{S}_2}(\mathbf{z})\cdot\mathbf{U}_{\mathcal{S}_3}(\mathbf{z}_0)\right]\ , \tag{33a}$$
$$= -\frac{1}{R^2}\sum_{l=1}^{\infty}\sum_{m=-l}^{+l}\frac{1}{l(l+1)}\nabla_{\mathcal{S}_3}\overline{Y}^m_l(\mathbf{z})\nabla_{\mathcal{S}_3}Y^m_l(\mathbf{z}_0)\ , \tag{33b}$$

as a short algebra will show. We stress that $\mathbf{G}^{\text{mono}}_0(M,M_0)$ is a $3D$ dyadic tensor of the type $\mathbf{A}(M)\mathbf{A}(M_0)$, $\mathbf{A}(M)$ and $\mathbf{A}(M_0)$ being two vectors tangent to the sphere at the points M and M_0, respectively. It is easy to show that in the limit $\psi_{M_0M}\to 0$, $\mathbf{G}^{\text{mono}}_0(M,M_0)$ tends to its Euclidian limit $\mathbf{G}_{0,E_2}(M,M_0) = [-\mathbf{U}_{E_2}(M) + 2\widehat{\boldsymbol{\rho}}\widehat{\boldsymbol{\rho}}]/(2\pi\rho^2)$, with $\boldsymbol{\rho} = \overrightarrow{M_0M}$ and $\widehat{\boldsymbol{\rho}} = \boldsymbol{\rho}/\rho$ and where $\mathbf{U}_{E_2}(M) = \mathbf{e}_\theta\mathbf{e}_\theta + \mathbf{e}_\varphi\mathbf{e}_\varphi$ is the unit dyadic tensor in the tangent plane $\mathcal{T}(M)$.

With arguments similar to those exposed in Ref. [17–19, 23] for the $3D$ case, one can easily show that the distribution $\mathbf{G}_{0,E_2}(M,M_0)$ has a singularity $-(1/2)\mathbf{U}\delta^{(2)}(\boldsymbol{\rho})$. Therefore $\mathbf{G}^{\text{mono}}_0(M,M_0)$ is singular for $\psi_{M_0M}\to 0$, with the same singularity. As for the $3D$ case [7] it

may be important to extract this singularity and to define a non-singular Green's function $\mathbf{G}_0^{\text{mono},\delta}(M, M_0)$ by the relations

$$\mathbf{G}_0^{\text{mono}}(M, M_0) = \mathbf{G}_0^{\text{mono},\delta}(M, M_0) - \frac{1}{2}\delta(M, M_0)\,\mathbf{U}_{\mathcal{S}_2}(\mathbf{z}) \;, \tag{34a}$$

$$\mathbf{G}_0^{\text{mono},\delta}(M, M_0) = \begin{cases} \mathbf{G}_0^{\text{mono}}(M, M_0) & , \text{ for } R\psi_{M_0 M} > \delta \;, \\ 0 & , \text{ for } R\psi_{M_0 M} < \delta \;, \end{cases} \tag{34b}$$

where δ is an arbitrary small cut-off ultimately set to zero. It must be understood that any integral involving $\mathbf{G}_0^{\text{mono},\delta}$ must be calculated with $\delta \neq 0$ and then taking the limit $\delta \to 0$. These matters are discussed in appendix A together with some other useful mathematical properties of $\mathbf{G}_0^{\text{mono}}(M, M_0)$.

For the bi-dipoles one finds

$$\begin{aligned} \mathbf{G}_0^{\text{bi}}(M, M_0) =& \mathbf{G}_0^{\text{mono}}(M, M_0) + \mathbf{G}_0^{\text{mono}}(M, \overline{M}_0) \\ =& \frac{1}{2\pi R^2}\frac{1}{\sin^2\psi_{M_0 M}} \qquad\qquad (35a) \\ & \left[2\cos\psi_{M_0 M}\mathbf{t}_{MM_0}(M)\mathbf{t}_{MM_0}(M_0) - \mathbf{U}_{\mathcal{S}_2}(\mathbf{z})\cdot\mathbf{U}_{\mathcal{S}_3}(\mathbf{z}_0)\right] \;, \qquad (35b) \\ =& -\frac{2}{R^2}\sum_{l \text{ odd}}\sum_{m=-l}^{+l}\frac{1}{l(l+1)}\nabla_{\mathcal{S}_3}\overline{Y}_l^m(\mathbf{z})\nabla_{\mathcal{S}_3}Y_l^m(\mathbf{z}_0) \;. \qquad (35c) \end{aligned}$$

in addition to a singularity for $M \to M_0$ (the same as that of $\mathbf{G}_0^{\text{mono}}(M, M_0)$) the Green's function $\mathbf{G}_0^{\text{bi}}(M, M_0)$ bears another singularity for $M \to \overline{M_0}$.

C. Dipole-dipole interaction

We end this section by *defining* the interaction of two dipoles $(M_1, \boldsymbol{\mu}_1)$ and $(M_2, \boldsymbol{\mu}_2)$ as $W_{\boldsymbol{\mu}_1,\boldsymbol{\mu}_2} \equiv -\boldsymbol{\mu}_1 \cdot 2\pi\mathbf{G}_0(1,2)\cdot\boldsymbol{\mu}_2$ which gives for the mono dipoles with the help of Eq. (33a)

$$W_{\boldsymbol{\mu}_1,\boldsymbol{\mu}_2}^{\text{mono}} = \frac{\mu^2}{2R^2}\frac{1}{1-\cos\psi_{12}}\left(\mathbf{s}_1\cdot\mathbf{s}_2 - (1+\cos\psi_{12})\,(\mathbf{t}_{12}(1)\cdot\mathbf{s}_1)(\mathbf{t}_{12}(2)\cdot\mathbf{s}_2)\right) \;, \tag{36a}$$

$$= \frac{\mu^2}{2R^2}\frac{1}{1-\cos\psi_{12}}\left(\mathbf{s}_1\cdot\mathbf{s}_2 + \frac{1}{1-\cos\psi_{12}}\,(\mathbf{s}_1\cdot\mathbf{z}_2)(\mathbf{s}_2\cdot\mathbf{z}_1)\right) \;, \tag{36b}$$

were we have adopted the simplified notation $\mathbf{t}_{12}(i) \equiv \mathbf{t}_{M_1M_2}(M_i)$ $(i = 1, 2)$ to denote the two unit vectors tangent to the geodesic $\overset{\frown}{M_1M_2}$. The interaction energy of two bi-dipoles is

given by

$$W^{\rm bi}_{\boldsymbol{\mu}_1,\boldsymbol{\mu}_2} = \frac{\mu^2}{R^2}\frac{1}{\sin^2\psi_{12}}\left(\mathbf{s}_1\cdot\mathbf{s}_2 - 2\cos\psi_{12}\,(\mathbf{t}_{12}(1)\cdot\mathbf{s}_1)(\mathbf{t}_{12}(2)\cdot\mathbf{s}_2)\right) , \tag{37a}$$

$$= \frac{\mu^2}{R^2}\frac{1}{\sin^2\psi_{12}}\left(\mathbf{s}_1\cdot\mathbf{s}_2 + \frac{2\cos\psi_{12}}{\sin^2\psi_{12}}\,(\mathbf{s}_1\cdot\mathbf{z}_2)(\mathbf{s}_2\cdot\mathbf{z}_1)\right) . \tag{37b}$$

One recovers the well-known Euclidian limit $W^{\rm mono}_{\boldsymbol{\mu}_1,\boldsymbol{\mu}_2} \sim W^{\rm bi}_{\boldsymbol{\mu}_1,\boldsymbol{\mu}_2} \sim (\mu^2/\rho_{12}^2)[\mathbf{s}_1\cdot\mathbf{s}_2 - 2(\mathbf{s}_1\cdot\widehat{\boldsymbol{\rho}}_{12})(\mathbf{s}_2\cdot\widehat{\boldsymbol{\rho}}_{12})]$ of the dipole-dipole interaction when $\psi_{12}\to 0$.

IV. THE $2D$ POLAR FLUID IN $\mathcal{S}_2(O,R)$.

A. Two equivalent models for the dipolar hard sphere fluid in $\mathcal{S}_2(O,R)$

A fluid of point dipoles is not stable and additional repulsive short range pair-potentials must be included in the model to ensure the existence of a thermodynamic limit. In this paper we consider only hard core repulsions and thus the DHS model. Two versions are possible in $\mathcal{S}_2(O,R)$ depending on whether mono- or bi-dipoles are involved [7].

1. Monodipoles

In this version the mono-dipoles are embedded in the center of hard disks lying on the surface of the sphere. In a given configuration, N point-dipoles $\boldsymbol{\mu}_i$ are located at points $\mathbf{OM}_i = R\mathbf{z}_i$ $(i=1,\ldots,N)$ of $\mathcal{S}_2(O,R)$ and the configurational energy reads

$$U(\{\mathbf{z}_i,\boldsymbol{\mu}_i\}) = \frac{1}{2}\sum_{i\neq j}^{N} v^{\rm mono}_{\rm HS}(\psi_{ij}) + \frac{1}{2}\sum_{i\neq j}^{N} W^{\rm mono}_{\boldsymbol{\mu}_i,\boldsymbol{\mu}_j} , \tag{38}$$

where $v^{\rm mono}_{\rm HS}(\psi_{ij})$ is the hard-core pair potential in $\mathcal{S}_2(O,R)$ defined by

$$v^{\rm mono}_{\rm HS}(\psi_{ij}) = \begin{cases} \infty & \text{if } \sigma/R > \psi_{ij} \ , \\ 0 & \text{otherwise} \ \ , \end{cases} \tag{39}$$

and $W^{\rm mono}_{\boldsymbol{\mu}_i,\boldsymbol{\mu}_j}$ is the energy of a pair of mono-dipoles given at Eq. (36). Note that the distance σ is measured along the geodesics and not in the Euclidian space E_3. The hard disks are in fact curved objects, similar to contact lenses at the surface of an eye-ball.

A thermodynamic state of this model is characterized by a density $\rho^* = N\sigma^2/S$ where $S = 4\pi R^2$ is the $2D$ surface of the sphere $\mathcal{S}_2(O,R)$ and a reduced dipole moment μ^* with $\mu^{*2} = \mu^2/(k_B T\sigma^2)$ (k_B Boltzmann constant, T absolute temperature).

2. Bi-dipoles

In the second version we consider a fluid of dipolar dumbells confined on the surface of the sphere $\mathcal{S}_2(O,R)$. Both dipoles of the dumbell are embedded at the center of a hard sphere of diameter σ. In a given configuration, N dipoles $\boldsymbol{\mu}_i$ are located at points $\mathbf{OM}_i = R\mathbf{z}_i$ and their N companions $\boldsymbol{\mu}_i$ at the antipodal points $\mathbf{O\overline{M}}_i = -R\mathbf{z}_i$ $(i = 1, \ldots, N)$ of $\mathcal{S}_2(O,R)$. Each pair constitute a bi-dipole and only one of the two dipoles lies in the Nothern hemisphere $\mathcal{S}_2(O,R)^+$. The configurational energy reads

$$U(\{\mathbf{z}_i, \boldsymbol{\mu}_i\}) = \frac{1}{2}\sum_{i\neq j}^{N} v_{\text{HS}}^{\text{bi}}(\psi_{ij}) + \frac{1}{2}\sum_{i\neq j}^{N} W_{\boldsymbol{\mu}_i,\boldsymbol{\mu}_j}^{\text{bi}} \ , \tag{40}$$

where $v_{\text{HS}}^{\text{bi}}(\psi_{ij})$ is hard-core pair potential defined by

$$v_{\text{HS}}^{\text{bi}}(\psi_{ij}) = \begin{cases} \infty & \text{if } \sigma/R > \psi_{ij} \text{ or } \psi_{ij} > \pi - \sigma/R \ , \\ 0 & \text{otherwise} \ , \end{cases} \tag{41}$$

and the dipole-dipole interaction $W_{\boldsymbol{\mu}_i,\boldsymbol{\mu}_j}^{\text{bi}}$ is that defined at Eq. (37). In Eq. (40) the vectors $\mathbf{z}_i$ can allways be chosen in the northern hemisphere $\mathcal{S}_2(O,R)^+$ because of the special symmetries of the interaction. Indeed it we have by construction $V_{M_i,\boldsymbol{\mu}_i}^{\text{bi}}(M) = V_{\overline{M}_i,\boldsymbol{\mu}_i}^{\text{bi}}(M)$ (cf Eq. (31b)) and $\mathbf{E}_{M_i,\boldsymbol{\mu}_i}^{\text{bi}}(M) = \mathbf{E}_{\overline{M}_i,\boldsymbol{\mu}_i}^{\text{bi}}(M)$ (cf Eq. (35a)) for any point M of $\mathcal{S}_2(O,R)^+$ and any configuration of bi-dipoles. It is thus clear that the genuine domain occupied by the fluid is the northern hemisphere $\mathcal{S}_2(O,R)^+$ rather than the whole hypersphere. The interpretation of the model is therefore the following. When a dipole $\boldsymbol{\mu}_i$ quits $\mathcal{S}_2(O,R)^+$ at some point M_i of the equator the same $\boldsymbol{\mu}_i$ reenters at the antipodal point $\overline{M}_i$. Therefore bi-dipoles living on the whole sphere are equivalent to mono-dipoles living on the northern hemisphere but with special boundary conditions ensuring homogeneity and isotropy at equilibrium (in the case of a fluid phase).

A thermodynamic state of this model is now characterized by a density $\rho^* = N\sigma^2/S$ where $S = 2\pi R^2$ is the $2D$ surface of the northern hemisphere $\mathcal{S}_2^+(O,R)$ and the reduced dipole μ^* with $\mu^{*2} = \mu^2/(k_B T\sigma^2)$ as in Sec. IV A 1.

B. Thermodynamic and structure

Most properties of the DHS fluid at thermal equilibrium can be obtained from the knowledge of the one- and two-body correlation functions defined on the sphere and in the canon-

ical ensemble as

$$\rho^{(1)}(1) = \left\langle \sum_{i=1}^{N} \delta(M_1, M_i)\, \delta(\alpha_1 - \alpha_i) \right\rangle \tag{42a}$$

$$\rho^{(2)}(1,2) = \left\langle \sum_{i=1}^{N} \sum_{j=1}^{N} (1-\delta_{ij}) \delta(M_1, M_i)\, \delta(M_2, M_j)\, \delta(\alpha_1 - \alpha_i)\, \delta(\alpha_2 - \alpha_j) \right\rangle . \tag{42b}$$

Here $(i) \equiv (\mathbf{z}_i, \alpha_i)$ denotes both the position $\mathbf{z}_i$ of dipole "i" and its orientation, specified by the angle α_i. This angle can be measured for instance in the local basis $(\mathbf{e}_{\theta_i},\ \mathbf{e}_{\varphi_i})$ of spherical coordinates, *i.e.* $\alpha_i = (\widehat{\mathbf{e}_{\theta_i}, \mathbf{s}_i})$. For a homogeneous and isotropic fluid one has $\rho^{(1)}(1) = \rho/(2\pi)$ where $\rho = N/S$ is the number density and

$$\rho^{(2)}(1,2) = \left(\frac{\rho}{2\pi}\right)^2 g(1,2) , \tag{43}$$

where the correlation function $g(1,2)$ has been normalized so as to tend to 1 at large distances. To exploit the symmetries of the fluid phase It is far more convenient to use, instead of the α_i, the angles $\beta_i = (\widehat{\mathbf{t}_{12}(i), \mathbf{s}_i})$ $(i = 1,2)$. In order to complete the local basis in the tangent planes $\mathcal{T}_i$ $(i = 1,2)$ one defines $\mathbf{n}_{12}(i) = \mathbf{z}_i \times \mathbf{t}_{12}(i)$ $(i = 1,2)$. Remarkably the vector $\mathbf{n}_{12}$ is invariant along the geodesic $\widehat{M_1 M_2}$ and one has

$$\mathbf{n}_{12}(i) \equiv \mathbf{n}_{12} = \frac{\mathbf{z}_1 \times \mathbf{z}_2}{\sin \psi_{12}} . \tag{44}$$

Note by passing that the unit dyadic tensor $\mathbf{U}_{\mathcal{S}_2}(\mathbf{z}_i) = \mathbf{n}_{12}\mathbf{n}_{12} + \mathbf{t}_{12}(i)\mathbf{t}_{12}(i)$ for $i = 1,2$.

These variables (β_1, β_2) serve mainly to introduce a basis of $2D$ rotational invariants $\Psi_{mn}(\beta_1, \beta_2)$ upon which to expand the pair correlation function $g(1,2)$. The rotational invariants were introduced by Blum and Toruella in the context of $3D$ homogeneous and isotropic molecular fluids [28] and their $2D$ counterparts in the $2D$ plane were given in Refs [4, 5]. On the sphere the extension of the latter result is straightforward and these invariants read

$$\Psi_{mn}(1,2) \equiv \exp\left(im\beta_1 + in\beta_2\right) . \tag{45}$$

These functions are indeed invariant under the action of a global rotation of E_3 of center O. Moreover these invariants are orthogonal is the sense that

$$< \Psi_{mn} | \Psi_{pq} > \equiv \int \frac{d\beta_1}{2\pi} \int \frac{d\beta_2}{2\pi} \overline{\Psi}_{mn}(1,2) \Psi_{pq}(1,2) = \delta_{mp}\delta_{nq} . \tag{46}$$

and in an homogeneous and isotropic phase of the DHS fluid one has the expansion

$$g(1,2) = \sum_{m,n=-\infty}^{\infty} g_{mn}(r_{12}) \Psi_{mn}(1,2) , \tag{47}$$

where the coefficients $g_{mn}(r_{12})$ are functions of the length $r_{12} = R\psi_{12}$ of the geodesic $\widehat{M_1 M_2}$.

Reality of the correlation function $g(1,2)$ and invariance through the reflexion $(\beta_1, \beta_2) \leftrightarrow (-\beta_1, -\beta_2)$ impose that $g_{mn} = g_{-m-n} = g^*_{mn}$. These conditions enable us to define the real rotational invariants

$$\begin{aligned} \Phi_{mn} &= \frac{1}{2}\left(\Psi_{mn} + \Psi_{-m-n}\right) \\ &= \cos\left(m\beta_1 + n\beta_2\right) \ . \end{aligned} \tag{48}$$

To give some physical and geometrical interpretation of some of these invariants we first recall the expression of the scalar product on the sphere $\mathcal{S}_n(O,R)$ [4–7]. Taking the scalar product $\Delta(1,2)$ of two vectors $\mathbf{s}_1$ and $\mathbf{s}_2$ located at two distinct points, M_1 and M_2 of $\mathcal{S}_2(O,R)$ needs some caution. It first requires to perform a parallel transport of vector $\mathbf{s}_1$ from M_1 to M_2 along the geodesic $\widehat{M_1 M_2}$ and then to take a 2D scalar product in space $\mathcal{T}(M_2)$. Thus

$$\Delta(1,2) = \tau_{12}\mathbf{s}_1 \cdot \mathbf{s}_2 \ , \tag{49}$$

where, in the r.h.s. the dot denotes the usual scalar product of the Euclidian space $\mathcal{T}(M_2)$. Vector $\tau_{12}\mathbf{s}_1$ results from a transport of $\mathbf{s}_1$ from the space $\mathcal{T}(M_1)$ to the space $\mathcal{T}(M_2)$ along the geodesic $M_1 M_2$, keeping its angle with the tangent to the geodesic constant. Explicitely one has:

$$\tau_{12}\mathbf{s}_1 = \mathbf{s}_1 - \frac{\mathbf{s}_1 \cdot \mathbf{z}_2}{1 + \cos\psi_{12}} \ (\mathbf{z}_1 + \mathbf{z}_2) \ , \tag{50}$$

and thus

$$\Delta(1,2) = \mathbf{s}_1 \cdot \mathbf{s}_2 - \frac{(\mathbf{s}_1 \cdot \mathbf{z}_2)(\mathbf{s}_2 \cdot \mathbf{z}_1)}{1 + \cos\psi_{12}} \ . \tag{51}$$

The above expression (51) is in fact valid for a hypersphere $\mathcal{S}_n(O,R)$ of arbitrary dimensions. In the case $n = 2$ more simple expressions can easily be obtained with the help of the angles β_i introduced previously. Starting from $\mathbf{s}_1 = \cos\beta_1 \mathbf{t}_{12}(1) + \sin\beta_1 \mathbf{n}_{12}$ one deduces from (50) that $\tau_{12}\mathbf{s}_1 = \cos\beta_1 \mathbf{t}_{12}(2) + \sin\beta_1 \mathbf{n}_{12}$ from which it follows that

$$\Delta(1,2) = \cos(\beta_1 - \beta_2) \ , \tag{52}$$

and therefore $\Delta \equiv \Phi_{1-1}$.

By analogy with the $2D$ Euclidian case we also introduce the manifestly rotationally

invariant function $D(1,2)$

$$
\begin{aligned}
D(1,2) &\equiv = 2\big(\mathbf{s}_1 \cdot \mathbf{t}_{12}(1)\big)\big(\mathbf{s}_2 \cdot \mathbf{t}_{12}(2)\big) - \Delta(1,2) \\
&= -\mathbf{s}_1 \cdot \mathbf{s}_2 - \frac{(\mathbf{s}_1 \cdot \mathbf{z}_2)(\mathbf{s}_2 \cdot \mathbf{z}_1)}{1 - \cos\psi_{12}} \ .
\end{aligned} \tag{53}
$$

An explicit calculation shows that in $\mathcal{S}_2(O,R)$ one also has

$$
D(1,2) = \cos(\beta_1 + \beta_2) \ , \tag{54}
$$

and therefore $D \equiv \Phi_{11}$.

The angular Dependance of the dipole-dipole interactions (36) and (37) should be rotationally invariant and indeed one finds that it is a combination of the invariants D and Δ. More precisely one has

$$
W^{\text{mono}}_{\boldsymbol{\mu}_1,\boldsymbol{\mu}_2} = -\frac{\mu^2}{R^2 \sin^2\psi_{12}} \frac{1+\cos\psi_{12}}{2} D(1,2) \tag{55a}
$$

$$
W^{\text{bi}}_{\boldsymbol{\mu}_1,\boldsymbol{\mu}_2} = -\frac{\mu^2}{R^2 \sin^2\psi_{12}} \left[\left(\frac{1+\cos\psi_{12}}{2}\right) D(1,2) - \left(\frac{1-\cos\psi_{12}}{2}\right) \Delta(1,2) \right] \ . \tag{55b}
$$

The expressions of the projection $g^{mn}(r_{12})$ of the pair correlation $g(1,2)$ on the rotational invariants are easily deduced from the definition (42b) of the two point function $\rho^{(2)}(1,2)$ and the properties of orthogonality of the Φ_{mn}. One finds (in the canonical ensemble)

$$
g^{mn}(r_{12}) = \frac{1}{\langle \Phi_{mn} | \Phi_{mn} \rangle} \frac{1}{N\rho} \left\langle \frac{\sum_{i \neq j} \Phi_{mn}(i,j) \chi(\psi_{ij} - \psi_{12})}{2\pi R^2 \sin(\psi_{ij}) \delta\psi} \right\rangle \ , \tag{56}
$$

where $\delta\psi$ is the bin size and χ is defined as

$$
\chi(\psi - \psi_{12}) = \begin{cases} 1 \ \text{ if } \psi_{12} < \psi < \psi_{12} + \delta\psi \\ 0 \ \text{ otherwise.} \end{cases} \tag{57}
$$

Note that $\langle D|D \rangle = \langle \Delta|\Delta \rangle = 1/2$ while $\langle \Phi^{00}|\Phi^{00} \rangle = 1$. We want to point out that for the DHS fluid of mono-dipoles $0 < \psi_{12} = r_{12}/R < \pi$, however, for the fluid of bi-dipoles, only the range $0 < \psi_{12} < \pi/2$ is available, because of the special boundary conditions involved in the model.

If follows from the precedent developments that, at equilibrium, the mean energy per par particles reads

$$
\begin{aligned}
\beta u^{\text{mono}} &\equiv \frac{< \sum_{i \neq j} W^{\text{mono}}_{\boldsymbol{\mu}_i,\boldsymbol{\mu}_j} >}{2N} \\
&= -\frac{y}{4} \int_0^{\pi} d\psi \, \sin\psi \frac{h^D(R\psi)}{1 - \cos\psi} \ ,
\end{aligned} \tag{58a}
$$

for mono-dipoles and

$$\beta u^{\mathrm{bi}} \equiv \frac{< \sum_{i\neq j} W^{\mathrm{mono}}_{\boldsymbol{\mu}_i,\boldsymbol{\mu}_j} >}{2N}$$
$$= -\frac{y}{4}\int_0^{\pi/2} d\psi \, \sin\psi \left[\frac{h^D(R\psi)}{1-\cos\psi} - \frac{h^\Delta(R\psi)}{1+\cos\psi}\right] \, , \tag{59a}$$

for bi-dipoles. In Eqs (58) and (58) we have introduced the dimensionless parameter $y = \pi\rho\beta\mu^2$ and $h \equiv g - 1$.

For the sake of exhaustivity we finally quote the expression of the compressibility factor

$$Z^{\mathrm{mono\,(bi)}} = 1 + \beta u^{\mathrm{mono\,(bi)}} + \frac{\pi}{2}\rho^* \left[\frac{R}{\sigma}\sin\frac{\sigma}{R}\right] g^{00}(\sigma+0) \, . \tag{60}$$

Note the prefactor of the isotropic projection $g^{00}(\sigma + 0)$ at contact which accounts for curvature effects. The usual Euclidian expression $Z_\infty = 1 + \beta u_\infty + (\pi\rho^*/2)g^{00}(\sigma+0)$ emerges in the limit $R \to \infty$, both for mono- and bi-dipoles, as it was expected.

C. Fulton's theory

Let us consider quite generally a polar fluid occupying a $2D$ surface Λ with boundaries $\partial\Lambda$. We assume the system at thermal equilibrium in a homogeneous and isotropic fluid phase. The fluid behaves macroscopically as a dielectric medium characterized by a dielectric constant ϵ. Due to the lack of screening in such fluids, the asymptotic behavior of the pair correlation function is long ranged and depends on the geometry of the system, *i.e.* its shape, size, and the properties imposed to the electric field (or potential) on the boundaries $\partial\Lambda$ as well. As a consequence, the expression of the dielectric constant ϵ in terms of the fluctuations of polarization also depends on the geometry. These issues can be formally taken into account in the framework of Fulton's theory [17–19] which achieves an elegant synthesis between the linear response theory and the electrodynamics of continuous media.

This formalism can be extended without more ado to non-euclidian geometries and was applied notably for $3D$ hyperspheres and cubico-periodical systems in Refs. [7, 29]. In this section it is applied to the $2D$ sphere both for mono- and bi-dipoles (a separate treatment of each model is however necessary). To our knowledge the case of the $2D$ plane E_2 was never considered in the framework of Fulton's theory and it is given a special treatment in appendix (B).

1. Mono-dipoles

We consider a fluid of N mono-dipoles in $\mathcal{S}_2(O, R)$ at thermal equilibrium in the presence of an external electrostatic field $\boldsymbol{\mathcal{E}}(M) \in \mathcal{T}(M)$. The medium acquires a macroscopic polarization

$$\mathbf{P}(M) = < \widehat{\mathbf{P}}(M) >_{\boldsymbol{\mathcal{E}}} , \tag{61}$$

where the brackets denote the equilibrium average of the microscopic polarization $\widehat{\mathbf{P}}(M)$ in the presence of the external field $\boldsymbol{\mathcal{E}}$. In $\mathcal{S}_2(O, R)$ the microscopic polarization $\widehat{\mathbf{P}}(M)$ is defined as [7, 29]

$$\widehat{\mathbf{P}}(M) = \sum_{j=1}^{N} \mathbf{U}_{\mathcal{S}_2}(\mathbf{z}) \cdot \boldsymbol{\mu}_j \, \delta(M, M_j) , \tag{62}$$

where the unit dyadic tensor $\mathbf{U}_{\mathcal{S}_2}(\mathbf{z})$ in the r.h.s. of Eq. (62) ensures that vector $\widehat{\mathbf{P}}(M)$ belongs to the plane $\mathcal{T}(M)$ tangent to the sphere at point M.

The relation between the macroscopic polarization $\mathbf{P}(M)$ and the external field $\boldsymbol{\mathcal{E}}(\mathbf{r})$ can be established in the framework of linear-response theory, provided that $\boldsymbol{\mathcal{E}}(M)$ is small enough, with the result

$$2\pi \mathbf{P}(M) = \boldsymbol{\chi} \circ \boldsymbol{\mathcal{E}} \left(\equiv \int_{\mathcal{S}_2(O,R)} dS' \; \boldsymbol{\chi}(M, M') \cdot \boldsymbol{\mathcal{E}}(M') \right) . \tag{63}$$

The r.h.s. of Eq. (63) has been formulated in a compact, albeit convenient notation that will be adopted henceforth, where the symbol $\circ$ means both a tensorial contraction (denoted by the dot " $\cdot$ ") and a spacial convolution over the whole sphere.

From standard linear response theory the tensorial susceptibility $\boldsymbol{\chi}$ is then given by

$$\boldsymbol{\chi}(M_1, M_2) = 2\pi\beta < \widehat{\mathbf{P}}(M_1)\widehat{\mathbf{P}}(M_2) > , \tag{64}$$

where the thermal average $< \ldots >$ in the r.h.s. of (64) is now evaluated in the absence of the external field, $\mathcal{E} \equiv 0$. The susceptibility tensor $\boldsymbol{\chi}(M_1, M_2)$ can be expressed in terms of the one- and two- point correlation functions (42) as

$$\boldsymbol{\chi}(M_1, M_2) = \boldsymbol{\chi}_S(M_1, M_2) + \boldsymbol{\chi}_D(M_1, M_2) , \tag{65}$$

where the "self" part reads

$$\boldsymbol{\chi}_S(M_1, M_2) = y \, \delta(M_1, M_2) \, \mathbf{U}_{\mathcal{S}_2}(\mathbf{z_1}) , \tag{66}$$

and

$$\boldsymbol{\chi}_D(M_1, M_2) = 2y\rho \int_0^{2\pi} \frac{d\beta_1}{2\pi} \int_0^{2\pi} \frac{d\beta_2}{2\pi} h(1,2)\mathbf{s}_1\mathbf{s}_2 \,. \tag{67}$$

After making use of the expansion (47) of $h(1,2)$ in rotational invariants one finds finally

$$\begin{aligned}
\boldsymbol{\chi}(M_1, M_2) = & \; y\delta\,(M_1, M_2)\; \mathbf{U}_{\mathcal{S}_2}\,(\mathbf{z_1}) \\
& + \frac{y\rho}{2} \left\{ \left[(1-\cos\psi_{12}) h^{\Delta}(r_{12}) + (1+\cos\psi_{12}) h^{D}(r_{12}) \right] \mathbf{t}_{12}(1)\mathbf{t}_{12}(2) \right. \\
& \left. + \left(h^{\Delta}(r_{12}) - h^{D}(r_{12}) \right) \mathbf{U}_{\mathcal{S}_2}(\mathbf{z_1}) \cdot \mathbf{U}_{\mathcal{S}_2}(\mathbf{z_2}) \right\} \;.
\end{aligned} \tag{68}$$

We point out that in the limit r_{12} fixed, $R \to \infty$ the above expressions reduces to that derived in Appendix B for the $2D$ euclidian space (*cf* Eq. (B6)).

The dielectric properties of the fluid are characterized by the dielectric tensor $\boldsymbol{\epsilon}$ which enters the constitutive relation

$$2\pi \mathbf{P} = (\boldsymbol{\epsilon} - \mathbf{I}) \circ \mathbf{E} \,, \tag{69}$$

where $\mathbf{E}$ denotes the Maxwell field and $\mathbf{I}(M_1, M_2) \equiv \mathbf{U}_{\mathcal{S}_2}(\mathbf{z}_1)\delta(M_1, M_2)$. The Maxwell field $\mathbf{E}(M)$ is the sum of the external field $\boldsymbol{\mathcal{E}}(M)$ and the electric field created by the macroscopic polarization of the fluid. Therefore one has

$$\mathbf{E} = \boldsymbol{\mathcal{E}} + 2\pi \mathbf{G}_0^{\text{mono}} \circ \mathbf{P} \,. \tag{70}$$

It is generally assumed that $\boldsymbol{\epsilon}$ is a local function, *i.e.* $\boldsymbol{\epsilon} = \epsilon \mathbf{I}$. More precisely, it is plausible -and we shall take it for granted- that $\boldsymbol{\epsilon}(M_1, M_2)$ is a short range function of the distance between the two points (M_1, M_2), at least for a homogeneous liquid, and one then defines

$$\epsilon \mathbf{U}_{\mathcal{S}_2}(\mathbf{z_1}) = \int_{\mathcal{S}_2(O,R)} dS_2 \; \boldsymbol{\epsilon}(M_1 M_2) \,. \tag{71}$$

In general $(\boldsymbol{\epsilon} - \mathbf{I}) \neq \boldsymbol{\chi}$ since the Maxwell field $\mathbf{E}(M)$ and the external field $\boldsymbol{\mathcal{E}}(M)$ do not coincide. The relation between the two fields is easily obtained from (70) and usually recast as [17–19, 29]

$$\mathbf{E} = \boldsymbol{\mathcal{E}} + \mathbf{G}^{\text{mono}} \circ \boldsymbol{\sigma} \circ \boldsymbol{\mathcal{E}} \,, \tag{72}$$

where $\boldsymbol{\sigma} \equiv \boldsymbol{\epsilon} - \mathbf{I}$ and $\mathbf{G}^{\text{mono}}(M_1, M_2)$ is the macroscopic dielectric Green's function defined by the identity

$$\mathbf{G}^{\text{mono}} = \mathbf{G}_0^{\text{mono}} \circ (\mathbf{I} - \boldsymbol{\sigma} \circ \mathbf{G}_0^{\text{mono}})^{-1} \,, \tag{73}$$

where the inverse must be understood in the sense of operators. It is easy to show that the electric field created at a point $M_1 \in \mathcal{S}_2(O, R)$ by a point mono-dipole $\boldsymbol{\mu}_2$ located at M_2 *in*

the presence of the dielectric medium is then given by $2\pi \mathbf{G}^{\rm mono}(M_1, M_2) \cdot \boldsymbol{\mu}_2$. This remark enlightens the physical meaning of the macroscopic Green's function.

Combining Eqs. (63), (69), and (72) yields Fulton's relation

$$\boldsymbol{\chi} = \boldsymbol{\sigma} + \boldsymbol{\sigma} \circ \mathbf{G}^{\rm mono} \circ \boldsymbol{\sigma} \ . \tag{74}$$

To go further one has to compute the macroscopic Green's function $\mathbf{G}^{\rm mono}$. Our starting point is the following identity, proved in appendix A :

$$\mathbf{G}_0^{\rm mono} \circ \mathbf{G}_0^{\rm mono} = -\mathbf{G}_0^{\rm mono} \ . \tag{75}$$

Therefore $-\mathbf{G}_0^{\rm mono}$ is a projector and has no inverse. Assuming the locality of $\boldsymbol{\sigma}$ one is then led to search the inverse $(\mathbf{I} - \boldsymbol{\sigma} \circ \mathbf{G}_0^{\rm mono})^{-1}$ in the r.h.s. of (73) under the form $a\mathbf{I} + b\mathbf{G}_0^{\rm mono}$ where a and b are numbers (or local operators). By identification one finds $a = 1$ and $b = \sigma/(1+\sigma)$ yielding for $\mathbf{G}^{\rm mono}$ the simple (and expected) expression

$$\mathbf{G}^{\rm mono} = \mathbf{G}_0^{\rm mono}/(1+\sigma) \equiv \mathbf{G}_0^{\rm mono}/\epsilon \ . \tag{76}$$

The results derived above allow us to recast Fulton's relation (74) under its final form

$$(\epsilon - 1)\mathbf{I}(M_1, M_2) + \frac{(\epsilon-1)^2}{\epsilon} \, \mathbf{G}_0^{\rm mono}(M_1, M_2) = \boldsymbol{\chi}(M_1, M_2) \ . \tag{77}$$

We stress that the above equation has been obtained under the assumption of the locality of the dielectric tensor $\boldsymbol{\epsilon}(M_1, M_2)$. Therefore it should be valid only asymptotically, *i.e.* for points (M_1, M_2) at a mutual distance r_{12} larger then the range ξ of $\boldsymbol{\epsilon}(M_1, M_2)$.

Expressions for the dielectric constant are obtained from Eq. (77) by space integration. Following Refs. [7, 29, 30] one integrates both sides of Eq. (77) and then takes the trace. The integration of M_2 is performed over a cone of axis $\mathbf{z}_1$ and aperture ψ_0 and then M_1 is integrated over the whole sphere $\mathcal{S}_2(O, R)$. The singularity of the dipolar Green's function $\mathbf{G}_0(M_1, M_2)$ for $\psi_{12} \sim 0$ must be carefully taken into account and this delicate point is detailed in appendix A (see Eq. (A9)). One finds finally

$$\frac{\epsilon - 1}{\epsilon} + \frac{(\epsilon-1)^2}{4\epsilon}(1 + \cos\psi_0) = \mathbf{m}^2(\psi_0) \ \text{ with } 0 < \psi_0 < \pi \ , \tag{78}$$

where the dipolar fluctuation $\mathbf{m}^2(\psi_0)$ reads as

$$\mathbf{m}^2(\psi_0) = \frac{\pi\beta\mu^2}{S} < \sum_i^N \sum_j^N \mathbf{s}_i \cdot \mathbf{s}_j \, \Theta(\psi_0 - \psi_{ij}) > , \tag{79}$$

where $\Theta(x)$ is the Heaviside step-function ($\Theta(x) = 0$ for $x < 0$ and $\Theta(x) = 1$ for $x > 0$).

We have thus obtained a family of formula depending on parameter $0 < \psi_0 < \pi$; clearly they should be valid only if $R\psi_0$ is large when compared to the range ξ of the dielectric constant. The numerical results of Sec. (V) show that this range is of the order of a few atomic diameters. It is also important to note that for $\psi_0 = \pi$ Eq. (78) involves the fluctuations of the total 3D dipole moment of the system. However, the resulting formula *i.e.* $(\epsilon - 1)/\epsilon = \mathbf{m}^2(\pi) = \pi\beta < \mathbf{M}^2 > /S$ (with $\mathbf{M} = \sum_i \boldsymbol{\mu}_i$ the total $3D$ dipole moment of the sphere), albeit simple, is not adapted for numerical applications since, for large values of the dielectric constant, a reasonable numerical error on ϵ requires a determination of $\mathbf{m}^2(\pi)$ with an impractical precision. The choice $\psi_0 = \pi/2$ yields the less simple formula $(\epsilon - 1)(\epsilon + 3)/\epsilon = 4\,\mathbf{m}^2(\pi/2)$ which however allows, by contrast, a precise determination of ϵ. Indeed, let $\delta\epsilon$ be the error on ϵ, then, for high values of the dielectric constant the errors on $\mathbf{m}^2(\pi/2)$ and ϵ are roughly proportional, *i.e.* $\delta\epsilon \sim 4\,\delta\mathbf{m}^2(\pi/2)$.

The fluctuation $\mathbf{m}^2(\psi_0)$ is related to the so-called Kirkwood factor $G^K(\psi_0)$. according to the relation $\mathbf{m}^2(\psi_0) = yG^K(\psi_0)$ with

$$G^K(r) = 1 + \rho\pi\, R^2 \int_0^{\psi_0} d\psi\ \sin\psi\, h^{\text{Kirk.}}(R\psi)\ , \tag{80}$$

where

$$h^{\text{Kirk.}}(r = R\psi) = \frac{1}{2}\,(1 + \cos\psi)h^{\Delta}(r) - \frac{1}{2}\,(1 - \cos\psi)h^{D}(r)\ . \tag{81}$$

Fulton's relation (77) can also be used to determine the asymptotic behavior of the projections $h^{\Delta}(r)$ and $h^{D}(r)$ the pair-correlation function $g(1,2)$. By comparing Eqs. (68) and (77) one obtains readily that, *asymptotically*, *i.e.* for large $r = R\psi$ and $\psi < \pi$, one has

$$h^{\Delta}_{\text{asymp.}}(r) \sim 0\ , \tag{82a}$$

$$h^{D}_{\text{asymp.}}(r) \sim \frac{(\epsilon - 1)^2}{y\rho\epsilon}\frac{1}{2\pi R^2}\frac{1}{1 - \cos\psi}\ , \tag{82b}$$

$$h^{\text{Kirk.}}_{\text{asymp.}}(r) \sim -\frac{(\epsilon - 1)^2}{y\rho\epsilon}\frac{1}{4\pi R^2} \tag{82c}$$

We note that $h^{\Delta}(r)$ has no tail and is thus a short-range function. It thus presents the same behavior as in the $2D$ Euclidean space (see Refs.[4, 5] and the new analysis in appendix B also based on Fulton's relation). We also note that, in the thermodynamic limit $R \to \infty$ *and* with $r \gg \xi$ fixed but large, one recovers the expected Euclidian behavior $h^{D}_{\text{asymp.}}(r) \sim (\epsilon - 1)^2/(\pi y\rho\epsilon) \times 1/r^2$ valid for an infinite system without boundaries at infinity(see *e.g.* [4, 5] and

Eq. (B12) of appendix B). The Kirkwood's function $h^{\text{Kirk.}}(r)$ exhibits a constant tail which tends to zero as the inverse of the surface $S = 4\pi R^2$ of the system. However the integration of this tail over the volume gives a non-zero contribution to the dielectric constant. In the limit $r = R\psi \gg \xi$ one has

$$\begin{aligned} G^K(\psi_0) &= G^K_\infty + \pi\rho R^2 \int_0^{\psi_0} d\psi \sin\psi \, h^{\text{Kirk.}}_{\text{asymp.}}(R\psi) \\ &= G^K_\infty - \frac{(\epsilon-1)^4}{4y\epsilon} \left(1 - \cos\psi_0\right) , \end{aligned} \tag{83}$$

where G^K_∞ is the Euclidian Kirkwood factor

$$G^K_\infty = 1 + \frac{\rho}{2} \int_0^\infty dr \, 2\pi r \, h^\Delta_\infty(r) , \tag{84}$$

where we have noted that, in the thermodynamic limit, r fixed and $R \to \infty$, $h^{\text{Kirk.}}(r) = h^\Delta_\infty(r)$. Reporting this asymptotic expression of the Kirkwood factor in Eq. (79) one recovers the formula valid for the Euclidian plane which reads as

$$\frac{(\epsilon-1)(\epsilon+1)}{2\epsilon} = y G^K_\infty . \tag{85}$$

which coincides with the Eq. (B10) obtained in the appendix B for the infinite plane E_2; note that Eq. 85 can be derived by a whole host of other methods, cf Refs [4, 5].

2. *Bi-dipoles*

The passage from mono- to bi-dipoles requires some adjustments. First, the appropriate bare Green's function is now $\mathbf{G}_0^{\text{bi}}$ as defined at Eqs. (35). Secondly the operation $\circ$ defined at Eq. (63) now involves a spacial integration the support of which is only the northern hemisphere $\mathcal{S}_2^+(O,R)$ rather than the entire surface of the sphere. For instance, as shown in appendix A one has

$$\begin{aligned} \left[\mathbf{G}_0^{\text{bi}} \circ \mathbf{G}_0^{\text{bi}}\right](M_1, M_2) &= \int_{\mathcal{S}_2^+(O,R)} dS \, \mathbf{G}_0^{\text{bi}}(M_1, M) \cdot \mathbf{G}_0^{\text{bi}}(M, M_2) \\ &= -\mathbf{G}_0^{\text{bi}}(M_1, M_2) \end{aligned} \tag{86}$$

for points points M_1 and M_2 belonging to the northern hemisphere. Therefore, reasoning as in Sec. IV C 1, we find for the dressed Green's function, asymptotically

$$\mathbf{G}^{\text{bi}} = \mathbf{G}_0^{\text{bi}} \circ \left(\mathbf{I} - \boldsymbol{\sigma} \circ \mathbf{G}_0^{\text{bi}}\right)^{-1} = \mathbf{G}_0^{\text{bi}}/\epsilon . \tag{87}$$

Clearly the susceptibility tensor $\boldsymbol{\chi}_D(M_1, M_2)$ keeps the same expressions (64) and (68) with the restriction that the two points M_1 and M_2 both belong to the northern hemisphere $\mathcal{S}_2^+(O,R)$. As in Sec. IV C 1 the dielectric constant can be obtained from Fulton's relation $\boldsymbol{\chi} = \boldsymbol{\sigma} + \boldsymbol{\sigma} \circ \mathbf{G}^{\text{bi}} \circ \boldsymbol{\sigma}$ and reads now

$$\frac{\epsilon - 1}{\epsilon} + \frac{(\epsilon-1)^2}{2\epsilon} \cos\psi_0 = \mathbf{m}^2(\psi_0) \quad \text{with } 0 < \psi_0 < \pi/2 \,, \tag{88}$$

where the fluctuation $\mathbf{m}^2(\psi_0)$ is still given by

$$\mathbf{m}^2(\psi_0) = \frac{\pi\beta\mu^2}{S} < \sum_i^N \sum_j^N \mathbf{s}_i \cdot \mathbf{s}_j \, \Theta(\psi_0 - \psi_{ij}) > \,, \tag{89}$$

but with $S = 2\pi R^2$ (surface of the northern hemisphere) and $0 < \psi_0 < \pi/2$. The delicate mathematical integration of the Green's function $\mathbf{G}^{\text{bi}}$ required to derive Eq. (89) is explained in appendix A.

We can note that for $\psi_0 = \pi/2$, *i.e.* when the fluctuation of the total dielectric moment of the sample is taken into account one still has $(\epsilon-1)/\epsilon = \pi\beta < \mathbf{M}^2 > /S$ with $\mathbf{M} = \sum_i \boldsymbol{\mu}_i$ the total $3D$ dipole moment of the northern hemisphere. Quite remarkably one obtains for $\psi_0 = \pi/3$ the relation $(\epsilon-1)(\epsilon+3)/\epsilon = 4\,\mathbf{m}^2(\pi/3)$ which is formally identical to that obtained for mono-dipoles with the choice $\psi_0 = \pi/2$. It is not a surprise since, in both cases, $\mathbf{m}^2(\psi_0)$ accounts for the dipole fluctuation of half the total domain available to the dipoles of the system.

The asymptotic behavior of the pair correlation function is obtained in the same vein as in Sec. IV C 1, *i.e.* for large $r = R\psi$ and $\psi < \pi/2$, one has

$$h^{\Delta}_{\text{asymp.}}(r) \sim -\frac{(\epsilon-1)^2}{y\rho\epsilon} \frac{1}{2\pi R^2} \frac{1}{1+\cos\psi} \,, \tag{90a}$$

$$h^{D}_{\text{asymp.}}(r) \sim \frac{(\epsilon-1)^2}{y\rho\epsilon} \frac{1}{2\pi R^2} \frac{1}{1-\cos\psi} \,, \tag{90b}$$

$$h^{\text{Kirk.}}_{\text{asymp.}}(r) \sim -\frac{(\epsilon-1)^2}{y\rho\epsilon} \frac{1}{2\pi R^2} \tag{90c}$$

In the limit $R \to \infty$ *and* with $r \gg \xi$ fixed but large, one recovers once again the expected Euclidian behavior $h^{D}_{\text{asymp.}}(r) \sim (\epsilon-1)^2/(\pi y\rho\epsilon) \times 1/r^2$. By contrast, in the same limit, one obtains that $h^{\Delta}_{\text{asymp.}}(r) \sim -(\epsilon-1)^2/(4\pi y\rho\epsilon) \times 1/R^2$ which tends to zero for the infinite system for which $R \to \infty$. This behavior is in agreement with the expected short range behavior of the projection $h^{\Delta}(r)$ in the $2D$ infinite Euclidian plane (cf Refs. [4, 5]

and the appendix B). The Kirkwood's function $h^{\mathrm{Kirk.}}_{\mathrm{asymp.}}(r)$ presents the same constant tail $-(\epsilon-1)^2/(y\rho\epsilon)\times 1/S$ as in the mono-dipole cases. Finally, in the thermodynamic limit, the Kirkwood's factor behaves as $G^K(\psi_0)=\mathbf{m}^2(\psi_0)/y=G^K_\infty-(\epsilon-1)^2\,(1-\cos\psi_0)/(2y\epsilon)$; by inserting this expression in Eq. (88) one recovers, as for mono-dipoles, the formula (85) valid for the Euclidian plane E_2.

V. SIMULATIONS

The only published MC simulations of the $2D$ DHS fluid the author is aware of are those of Morriss and Perram [21] published 30 years ago. Their simulation cell is a square with periodic boundary conditions and the authors make a correct use of Ewald dipolar potentials (an alternative version of that used in their paper, however non implemented in actual numerical simulations, is discussed in Ref. [22]). We have retained one of their points, *i.e.* our state I : ($\rho^*=0.7$, $\mu^{*2}=2$) as a benchmark. We also report MC data for a second reference state, our state II $\equiv$ ($\rho^*=0.6$, $\mu^{*2}=4$) characterized by a much higher dielectric constant. Both states undoubtly belongs to a stable fluid phase as it will be discussed below.

We performed standard MC simulations of a DHS fluid in the canonical ensemble with single particle displacement moves (translation and rotation). Each new configuration is thus generated by the trial displacement of *a randomly chosen single* dipole by means of a new algorithm explained in appendix C.

We considered both mono- and bi-dipoles on the sphere and studied finite size effects on the thermodynamic, structural and dielectric properties of the fluid. We studied systems of $N=250,500,1000,2000,$ and 4000 particles and typically we generated $N_{\mathrm{Nconf}}=16\,10^9$ configurations for each considered state.

Our results are resumed in Table I (state I) and Table II (state II). The errors reported in these tables correspond to two standard deviations in a standard statistical block analysis of the MC data [31].

As apparent in Fig. 1 the reduced internal βu energies converge linearly with $1/N$ to their thermodynamic limit βu_∞ for systems involving more than $N=250$ particles. This is true for systems of mono- and bi-dipoles. This allows a determination of βu_∞ with a precision of $\sim 3\,10^{-5}$. The asymptotic values obtained for mono- and bi-dipoles are identical within the error bars. Clearly the convergence towards the thermodynamic limit is faster for

bi-dipoles. Probably because, for a given density and number of particles, the radius R of the sphere is $\sqrt{2}$ larger for a system of bi-dipoles and therefore curvature effects are smaller. We note that our finding $\beta u_\infty = -1.79002 \pm 5 10^{-5}$ compares reasonably well with that obtained by Morriss and Perram for samples of $N = 100$ particles which lie in the interval $-1.795 < \ldots < -1.780$ depending on the type of boundaries surrounding the system at infinity [21].

Size effects on the short range part of the projections $g^{00}(r)$, $h^D(r)$, and $h^\Delta(r)$ are very small and cannot be appreciated on the graphs of the functions. To give an idea of these effects we give the contact value of these three projections in the tables. These values, which result from a Lagrange's polynomial interpolation, are much less precise than the values obtained for the energy. The compressibility factors Z were deduced from Eq. (60) and are also reported in the tables. The thermodynamic limit of these quantities do not seem to obey a simple linear regression with $1/N$. However, the low precision on the contact value $g^{00}(\sigma)$ precludes an unambiguous study of the thermodynamic limit in this case. We can infer from our MC data that, for state I one has in the thermodynamic limit $Z_\infty = 3.98 \pm 0.01$ a value once again not far from that of Ref. [21] $Z \sim 4.06$ obtained for a small system of a $N = 100$ dipoles.

The dielectric constants were obtained from Eq. (79) with $\psi_0 = \pi/2$ for mono-dipoles and from Eq. (89) with $\psi_0 = \pi/3$ for dipoles. As apparent on Figs. 2 the numerical uncertainties on ϵ are large and seem even to increase with system size but do not mask significant finite size effects. As for the pressure, it was impossible to deduce from our MC data a convergence law of $\epsilon(N)$ for $N \to \infty$ despite the huge number of MC steps involved. However we can claim that, for state I one has $\epsilon_\infty = 18.0 \pm 0.2$, which differs significantly from the value reported by Morriss and Perram $\epsilon = 16.0 \pm 0.5$.

In order to test the validity of Fulton's theory one can examine Fig. 3 which displays the Kirkwood factor $G^K(r)$ as a function of the distance $r = R\psi_0$ which defines the radius of the cap where the partial electric moment fluctuations are taken into account. As discussed in Sec. IV C, for $r > \xi$ (ξ range of the dielectric tensor) this function should be given by the asymptotic behaviors given by Eq. (78) for mono-dipoles and Eq. (88) for bi-dipoles. The dielectric constant used for these asymptotic forms are those given in Tables I and II. The excellent agreement beetween the MC data for $G^K(r)$ and the theoretical predictions even yields an estimation for the parameter ξ, i.e. $\xi \sim 7\sigma$ for both states I and II..

We check in Fig. 4 that the asymptotic behavior of the projection $h^{\Delta}(r)$ is indeed governed by the law of macroscopic electrostatics in $\mathcal{S}_2$, *i.e* by Eqs. (82) for mono-dipoles and Eqs. (90) for bi-dipoles. In all cases for $r > \xi$ the asymptotic behavior of $h^{\Delta}(r)$ is in excellent agreement with the theoretical prediction. Note that for mono-dipoles $h^{\Delta}(r)$ has no tail as expected from our theoretical developments. In the same vein Fig. 5 displays the ratio $h^D(r)/h^D_{\text{asymp.}}(r)$ for states I and II and several system sizes. Once again a satisfactory agreement simulation/theory can be observed. Note that for mono-dipoles (top curves) the noisy behavior at large distances is a consequence of the divergence (due to an insufficient sampling) of the term $\sim 1/\sin\psi_{ij}$ for $\psi_{ij} \sim \pi$ in the l.h.s. of Eq (56) which defines $h^D(r = R\psi)$ as a statistical average.

The fact that, for both states I and II, the theoretical asymptotic behavior of $h^{\Delta}(r)$ and $h^D(r)$ is reproduced by the MC data is a clue that the system is in an isotropic liquid phase. At lower temperatures chains of dipoles, rings, and topologically complex arrangements arise and the dielectric tensor either does not exist or is no more local. This point will be discussed elsewhere.

VI. CONCLUSION

In this work we have clarified the laws of electrostatics on the sphere $\mathcal{S}_2(0, R)$ by introducing two types of basic elements : pseudo- and bi-charges from which two types of multipoles can be obtained : mono- and bi-multipoles respectively. The electrostatic potentials of these multipoles can be obtained explicitely and exhaust all possible solutions of Laplace-Beltrami equation.

The application to polar fluids has been discussed in depth. Such a fluid can be represented either as an assembly of mono-dipoles living in $\mathcal{S}_2(0, R)$ or as a collection of bi-dipoles living in the northern hemisphere $\mathcal{S}_2(0, R)^+$.

Since the dipolar Green's function are explicitely known for both mono- and bi-dipoles, Fulton's theory of dielectric fluids can be explicitely worked out in the two cases. This includes the theory of the dielectric constant of an homogeneous and isotropic fluid and the derivation of the asymptotic tails of the projections $h^{\Delta}(r)$ and $h^D(r)$ of the equilibrium pair correlation function. It is likely that a violation of these asymptotic laws signals a phase transition towards a non-fluid phase.

We have reported and discussed MC simulations of two states of the DHS fluid which are both in the fluid phase and can serve as benchmark for future numerical works. Finite size effects have been studied and allow to reach, at least for the internal energy, the thermodynamic limit with a high precision ($\sim 10^{-5}$). Such a precision is smaller than the precision which could reasonably be obtained on the dipolar Ewald potential and *a fortiori* on the mean internal energy which could be computed by an actual MC simulation which would make use of it. This suggests that $\mathcal{S}_2(0, R)$ is a good geometry for precise MC simulations of the fluid phase. Simulations involving bi-dipoles appear to attain more quickly the thermodynamic limit than simulations involving mono-dipoles. An exploration of the phase diagram of the $2D$ DHS fluid will be presented elsewhere.

Acknowledgments

The author thanks Jean-Jacques Weis and Martin Trulsson for interesting discussions.

Appendix A: Mathematical properties of the dipolar Green's functions in $\mathcal{S}_2$

1. Convolutions

First we consider the case of mono-dipoles. Let $\mathbf{z}_1$ and $\mathbf{z}_2$ be two points of the sphere $\mathcal{S}_2$, we will show that

$$\begin{aligned}\mathbf{G}_0^{\mathrm{mono}} \circ \mathbf{G}_0^{\mathrm{mono}}(\mathbf{z}_1, \mathbf{z}_2) &\equiv \int_{\mathcal{S}_2} d\,\Omega(\mathbf{z}_3)\; \mathbf{G}_0^{\mathrm{mono}}(\mathbf{z}_1, \mathbf{z}_3) \cdot \mathbf{G}_0^{\mathrm{mono}}(\mathbf{z}_3, \mathbf{z}_2) \\ &= -\mathbf{G}_0^{\mathrm{mono}}(\mathbf{z}_1, \mathbf{z}_2)\;, \end{aligned} \tag{A1}$$

which shows that $-\mathbf{G}_0^{\mathrm{mono}}$ is a projector and has thus no inverse with respect to the binary operator " $\circ$ ". In order to prove Eq. (A1) we rewrite the expansion (33b) of the dipolar Green's function in spherical harmonics as

$$\mathbf{G}_0^{\mathrm{mono}}(\mathbf{z}_1, \mathbf{z}_2) = \sum_{l=1}^{\infty} \mathbf{G}_0^{l}(\mathbf{z}_1, \mathbf{z}_2)\;, \tag{A2}$$

with

$$\mathbf{G}_0^{l}(\mathbf{z}_1, \mathbf{z}_2) = -\frac{1}{l(l+1)} \sum_{m=-l}^{+l} \nabla_{\mathcal{S}_2} \overline{Y}_l^m(\mathbf{z}_1) \nabla_{\mathcal{S}_2} Y_l^m(\mathbf{z}_2)\;. \tag{A3}$$

To make further progress we need apply Green-Beltrami theorem in $\mathcal{S}_2$ which states that [25] :

$$\int_{\mathcal{S}_2} d\Omega \, \nabla_{\mathcal{S}_2} f \cdot \nabla_{\mathcal{S}_2} g = - \int_{\mathcal{S}_2} d\Omega \; f \Delta_{\mathcal{S}_3} g \; , \tag{A4}$$

where $f(\mathbf{z})$ and $g(\mathbf{z})$ are functions defined on the unit sphere $\mathcal{S}_2$. The proof of theorem (A4) is not so difficult and can be found, *e.g.* in the recent textbook by Atkinson and Han [25]. It follows from Eq. (A4) and the properties of spherical harmonics that

$$[\mathbf{G}_0^l \circ \mathbf{G}_0^p](\mathbf{z}_1, \mathbf{z}_2) = -\delta_{l,p} \, \mathbf{G}_0^l(\mathbf{z}_1, \mathbf{z}_2) \; , \tag{A5}$$

from which the identity (A1) is readily obtained.

The case of bi-dipoles is slightly different and has already been discussed in Ref. [7] for the $3D$ hyper-sphere $\mathcal{S}_3$. We now consider two points $\mathbf{z}_1$ and $\mathbf{z}_2$ of the northern hemisphere $\mathcal{S}_2^+$. We will show that, again

$$\begin{aligned} \mathbf{G}_0^{\mathrm{bi}} \circ \mathbf{G}_0^{\mathrm{bi}}(\mathbf{z}_1, \mathbf{z}_2) \equiv & \int_{\mathcal{S}_2^+} d\,\Omega(\mathbf{z}_3) \; \mathbf{G}_0^{\mathrm{bi}}(\mathbf{z}_1, \mathbf{z}_3) \cdot \mathbf{G}_0^{\mathrm{bi}}(\mathbf{z}_3, \mathbf{z}_2) \\ & = -\mathbf{G}_0^{\mathrm{bi}}(\mathbf{z}_1, \mathbf{z}_2) \; . \end{aligned} \tag{A6}$$

Note that, in this case, the space integration is restricted to the northern hemisphere. We follow the same strategy as for mono-dipoles and start with the expansion (35c) of the dipolar Green's function $\mathbf{G}_0^{\mathrm{bi}}(\mathbf{z}_1, \mathbf{z}_2)$ in spherical harmonics

$$\mathbf{G}_0^{\mathrm{bi}}(\mathbf{z}_1, \mathbf{z}_2) = 2 \sum_{l \; odd} \mathbf{G}_0^l(\mathbf{z}_1, \mathbf{z}_2) \; . \tag{A7}$$

For an odd value of l we have $Y_l^m(-\mathbf{z}) = -Y_l^m(\mathbf{z})$ which implies that

$$\mathbf{G}_0^l \circ \mathbf{G}_0^p(\mathbf{z}_1, \mathbf{z}_2) = -\frac{1}{2} \, \delta_{l,p} \, \mathbf{G}_0^l(\mathbf{z}_1, \mathbf{z}_2) \; , \tag{A8}$$

from which Eq. (A6) follows.

In this Sec. A 1 we implicitely assumed that $R = 1$. The reassessment of Eqs. (A1) and (A6) in the case $R \neq 1$ is however trivial since the mono and bi dipolar Green's function $\mathbf{G}_0(1, 2)$ scales as R^{-2} with the radius of the sphere. Clearly Eqs. (A1) and (A6) remain valid for $R \neq 1$ with the replacement $d\Omega(\mathbf{z}) \to dS(M)$.

2. Integration over cones

This section is devoted the integration of $\mathbf{G}_0^{\rm mono}(\mathbf{z}_1, \mathbf{z}_2)$ on a cone of axis $\mathbf{z}_1$ and aperture $0 \leq \psi_0 \leq \pi$. We shall prove that

$$\int_{0\leq\psi_{12}\leq\psi_0} d\,\Omega(\mathbf{z}_2)\ \mathbf{G}_0^{\rm mono}(\mathbf{z}_1, \mathbf{z}_2) = \frac{\cos\psi_0 - 3}{4}\,\mathbf{U}_{\mathcal{S}_2}(\mathbf{z}_1)\ . \tag{A9}$$

where $\psi_{12} = \cos^{-1}(\mathbf{z}_1 \cdot \mathbf{z}_2)$ is the angle between the two unit vectors $\mathbf{z}_1$ and $\mathbf{z}_2$. To prove Eq. (A9) one needs to take some precaution because of the singularity of $\mathbf{G}_0^{\rm mono}(\mathbf{z}_1, \mathbf{z}_2)$ at $\psi_{12} \to 0$. We make use of the decomposition (34a) to rewrite

$$\int_{0\leq\psi_{12}\leq\psi_0} d\,\Omega(\mathbf{z}_2)\ \mathbf{G}_0^{\rm mono}(\mathbf{z}_1, \mathbf{z}_2) = -\frac{1}{2}\mathbf{U}_{\mathcal{S}_2}(\mathbf{z}_1) + \lim_{\delta\to 0}\int_{\delta\leq\psi_{12}\leq\psi_0} d\,\Omega(\mathbf{z}_2)\ \mathbf{G}_0^{\rm mono}(\mathbf{z}_1, \mathbf{z}_2)\,. \tag{A10}$$

The integral $\mathbf{I}_\delta^{\psi_0}$ in the r.h.s. of Eq. (A10) is computed by using spherical coordinates to reexpress the formula (33b) of the Green function and performing explicitely the integrals. One has

$$\mathbf{G}_0^{\rm mono}(\mathbf{z}_1, \mathbf{z}_2) = \frac{1}{4\pi}\left\{\frac{1+\cos\psi_{12}}{1-\cos\psi_{12}}\mathbf{t}_{12}(\mathbf{z}_1)\mathbf{t}_{12}(\mathbf{z}_2) - \frac{1}{1-\cos\psi_{12}}\mathbf{U}_{\mathcal{S}_2}(\mathbf{z_1})\cdot\mathbf{U}_{\mathcal{S}_2}(\mathbf{z_2})\right\}$$

By taking the north pole at point $\mathbf{z}_1$ we have the identifications $\psi_{12} \to \theta$, $\mathbf{t}_{12}(\mathbf{z}_2) \to \mathbf{e}_\theta(\theta, \varphi)$ and $\mathbf{t}_{12}(\mathbf{z}_1) \to \mathbf{e}_\theta(\theta = 0, \varphi) = (\cos\varphi, \sin\varphi, 0)^T$. Therefore

$$\begin{aligned}
\mathbf{I}_\delta^{\psi_0} &= \frac{1}{4\pi}\int_\delta^{\psi_0}\sin\theta d\theta\int_0^{2\pi} d\varphi\left\{\frac{1+\cos\theta}{1-\cos\theta}\,\mathbf{e}_\theta(\theta,\varphi)\mathbf{e}_\theta(0,\varphi)\right.\\
&\quad\left. - \frac{1}{1-\cos\theta}\mathbf{U}_{\mathcal{S}_2}(0,\varphi)\cdot\mathbf{U}_{\mathcal{S}_2}(\theta,\varphi)\right\}\\
&= \frac{\cos\psi_0 - \cos\delta}{4}\mathbf{U}_{\mathcal{S}_2}(\mathbf{z_1})\ .
\end{aligned} \tag{A11}$$

Taking the limit $\delta \to 0$ and gathering the intermediate results (A10) and (A11) one obtains the desired result (A9).

The same type of calculation yields, for bi-dipoles,

$$\int_{0\leq\psi_{12}\leq\psi_0} d\,\Omega(\mathbf{z}_2)\ \mathbf{G}_0^{\rm bi}(\mathbf{z}_1, \mathbf{z}_2) = (\frac{\cos\psi_0}{2} - 1)\,\mathbf{U}_{\mathcal{S}_2}(\mathbf{z}_1)\ . \tag{A12}$$

with the restriction that $0 \leq \psi_0 \leq \pi/2$.

Appendix B: Fulton's theory in the plane.

In this section the domain occupied by the fluid consists of the entire $2D$ Euclidian plane E_2 with no boundaries at infinity. We consider Fulton relation (74) in this geometry. The susceptibility tensor $\boldsymbol{\chi}(M_1, M_2)$ at thermal equilibrium is

$$\boldsymbol{\chi}(M_1, M_2) = 2\pi\beta\mu^2 \, \langle \sum_{i,j} \mathbf{s}_i \mathbf{s}_j \, \delta^{(2)} \left(\mathbf{r}_1 - \mathbf{r}_i\right) \delta^{(2)} \left(\mathbf{r}_2 - \mathbf{r}_j\right) \rangle \; , \tag{B1a}$$

$$= \boldsymbol{\chi}_S(\mathbf{r}_{12}) + \boldsymbol{\chi}_D(\mathbf{r}_{12}) \; , \tag{B1b}$$

where $\overrightarrow{OM_i} = \mathbf{r}_i = (x_i, y_i)^T$ and $\mathbf{r}_{12} = \mathbf{r}_2 - \mathbf{r}_1$. The self-part $\boldsymbol{\chi}_S$ in (B1b) reads

$$\boldsymbol{\chi}_S(\mathbf{r}_{12}) = y \mathbf{I}(\mathbf{r}_1, \mathbf{r}_2) \; , \tag{B2}$$

with $y = \pi\rho\beta\mu^2$ and $\mathbf{I}(\mathbf{r}_1, \mathbf{r}_2) = \mathbf{U}\delta^{(2)}(\mathbf{r}_{12})$ where $\mathbf{U} = \mathbf{e}_x\mathbf{e}_x + \mathbf{e}_y\mathbf{e}_y$ is the unit dyadic tensor in E_2.

The contribution $\boldsymbol{\chi}_D$ to Eq. (B1b) can be expressed in terms of the pair correlation function $\rho^{(2)}(1,2) \equiv \rho^{(2)}(\mathbf{r}_1, \alpha_1; \mathbf{r}_2, \alpha_2)$ as

$$\boldsymbol{\chi}_D(\mathbf{r}_{12}) = 2\pi\beta\mu^2 \int_0^{2\pi} d\alpha_1 \int_0^{2\pi} d\alpha_2 \, \rho^{(2)}(1,2) \, \mathbf{s}_1 \mathbf{s}_2 \; . \tag{B3}$$

For a homogeneous and isotropic fluid $\rho^{(2)}(1,2) = (\rho/2\pi)^2 g(1,2)$. The normalized pair correlation function $g(1,2)$ can then be expanded on the complete set of $2D$ orthogonal rotational invariants as in Refs [4, 5]

$$h(1,2) = g(1,2) - 1 = \sum_{m,n} h_{m,n}(r_{12}) \Phi_{mn}(1,2) \; , \tag{B4}$$

where

$$\Phi_{mn}(1,2) = \cos(m\beta_1 + n\beta_2) \; . \tag{B5}$$

$\beta_1 = \alpha_1 - \theta_{12}$ and $\beta_2 = \alpha_2 - \theta_{12}$ are the angles of the vectors $\mathbf{s}_1$ and $\mathbf{s}_1$ and the direction $\mathbf{r}_{12}$ [4, 5] and the coefficients $h_{m,n}(r_{12})$ depends only on the sole modulus $r_{12} = \| \mathbf{r}_{12} \|$. The two invariants $D(1,2) \equiv \Phi_{11}(1,2)$ (minus the angular part of the dipole-dipole energy in the plane E_2) and $\Delta(1,2) \equiv \Phi_{1-1}(1,2)$ (scalar product $\mathbf{s}_1 \cdot \mathbf{s}_2$) play an important role since we have, as a short calculation will show

$$\boldsymbol{\chi}_D(\mathbf{r}_{12}) = \frac{\pi\beta\rho^2\mu^2}{2} \left[h^{\Delta}(_{12})\mathbf{U} + h^D(r_{12}) \left(2\widehat{\mathbf{r}}_{12}\widehat{\mathbf{r}}_{12} - \mathbf{U}\right) \right]$$

where $\widehat{\mathbf{r}}_{12} = \mathbf{r}_{12}/r_{12}$. Gathering the intermediate results we obtain

$$\boldsymbol{\chi}(\mathbf{r}_{12}) = y\mathbf{I}(\mathbf{r}_{12}) + \frac{y\rho}{2} h^{\Delta}(r_{12})\mathbf{U} + \frac{y\rho}{2} h^{D}(r_{12}) \left(2\widehat{\mathbf{r}}_{12}\widehat{\mathbf{r}}_{12} - \mathbf{U} \right) \ . \tag{B6}$$

We turn now our attention to the dipolar Green's functions in E_2. The bare Green's function is given by

$$\begin{aligned} \mathbf{G}_0(\mathbf{r}_1, \mathbf{r}_2) &= \frac{1}{2\pi} \frac{\partial}{\partial \mathbf{r}_1} \frac{\partial}{\partial \mathbf{r}_2} \log r_{12} \ , \\ &= \frac{1}{2\pi} \frac{1}{r_{12}^2} \left(2\widehat{\mathbf{r}}_{12}\widehat{\mathbf{r}}_{12} - \mathbf{U} \right) \ . \end{aligned} \tag{B7}$$

It is important to remark that Eq. (B7) implies that

$$\mathrm{Tr}\, \mathbf{G}_0(\mathbf{r}_1, \mathbf{r}_2) = \frac{1}{2\pi} \Delta(-\log r_{12}) = -\delta^{(2)}(\mathbf{r}_{12}) \ . \tag{B8}$$

We note that in Fourier space $\widetilde{\mathbf{G}}_0 = -\widehat{\mathbf{k}}\widehat{\mathbf{k}}$ (with $\widehat{\mathbf{k}} = \mathbf{k}/k$) identifies with minus the projector $\mathbf{P}_k \equiv \widehat{\mathbf{k}}\widehat{\mathbf{k}}$ on longitudinal modes. Denoting by $\mathbf{Q}_k = \mathbf{U} - \mathbf{P}_k$ the projector on tranverse modes one has the relations $\mathbf{P}_k \cdot \mathbf{P}_k = \mathbf{P}_k$, $\mathbf{Q}_k \cdot \mathbf{Q}_k = \mathbf{Q}_k$ and $\mathbf{P}_k \cdot \mathbf{Q}_k = 0$ from which the identity $(a\mathbf{P}_k + b\mathbf{Q}_k)^{-1} = a^{-1}\mathbf{P}_k + b^{-1}\mathbf{Q}_k$ can be deduced. Assuming the locality of dielectric tensor is local, *i.e.* $\widetilde{\boldsymbol{\epsilon}} = \epsilon\mathbf{U}$ in Fourier space, permits to compute the dressed Green's function $\widetilde{\mathbf{G}}$. One gets, as expected,

$$\widetilde{\mathbf{G}} = -\mathbf{P}_k \cdot \left[(1+\sigma)\, \mathbf{P}_k + \sigma \mathbf{Q}_k \right]^{-1} = \frac{\widetilde{\mathbf{G}}_0}{\epsilon} \tag{B9}$$

In order to obtain an expression for the dielectric constant we take the trace of both sides of Fulton's relation (74) and integrate over the whole plane. Making use of the expressions (B6) for $\boldsymbol{\chi}$ and the formula (B8) of the trace of $\mathbf{G}_0$ one finds

$$\frac{(\epsilon-1)(\epsilon+1)}{2\epsilon} = y\left(1 + \frac{\rho}{2} \int_0^{\infty} 2\pi r h_{\Delta}(r) dr \ \right) \tag{B10}$$

Fulton's relation (74) gives asymptotically (*i.e.* for $r_{12} >> \xi$, range of the dielectric tensor)

$$\boldsymbol{\chi}(\mathbf{r}_{12}) \simeq \frac{(\epsilon-1)^2}{\epsilon} \frac{1}{2\pi r_{12}^2} \left(2\widehat{\mathbf{r}}_{12}\widehat{\mathbf{r}}_{12} - \mathbf{U} \right) \ . \tag{B11}$$

A comparison of the above expression with Eq. (68) yields readily the asymptotic behaviors of $h_D(r)$ and $h_{\Delta}(r$:

$$h_{\Delta}^{\text{asym.}}(r) = 0 \ , \tag{B12a}$$

$$h_{D}^{\text{asym.}}(r) = \frac{(\epsilon-1)^2}{\epsilon} \frac{1}{\pi\rho y} \frac{1}{r^2} \ . \tag{B12b}$$

from which we conclude that, while $h_\Delta^{\text{asym.}}(r)$ is a short range function, the projection $h_D^{\text{asym.}}(r)$ exhibits a long range algebraic asymptotic decay. The results obtained in this appendix were obtained by other methods in Refs. [4, 5].

Appendix C: Dipole displacements on the sphere $\mathcal{S}_2$

The algorithm devised below adapts to the $2D$ case the algorithm used in Ref. [32] for the $3D$ DHS fluid on the hypersphere $\mathcal{S}_3$. The initial configuration of the Markov chain is obtained by sampling N vectors $\mathbf{z}^i$ uniformly on the sphere $\mathcal{S}_2$. The initial positions of the point dipoles are thus $\mathbf{OM}^i = R\mathbf{z}^i$. One uses the spherical coordinates in the base $(\mathbf{e}_x, \mathbf{e}_y, \mathbf{e}_z)$, *i.e.* $\mathbf{z}^i = (\sin\theta^i\cos\varphi^i, \sin\theta^i\sin\varphi^i, \cos\theta^i)^T$ with $\cos\varphi^i = 2\xi_1^i - 1$ and $\varphi^i = 2\pi\xi_2^i$ where ξ_1^i and ξ_2^i are $2N$ random numbers $\in (0,1)$. It is convenient to complete the orthogonal local basis of spherical coordinates at point M^i by defining also $\mathbf{u}^i = \partial\mathbf{z}^i/\partial\theta^i = (\cos\theta^i\cos\varphi^i, \cos\theta^i\sin\varphi^i, -\sin\theta^i)^T$ and $\mathbf{v}^i = \partial\mathbf{z}^i/\partial\varphi^i/\sin\theta^i = (-\sin\varphi^i, \cos\varphi^i, 0)^T$. The initial dipole $\boldsymbol{\mu}^i = \mu\mathbf{s}^i$ is randomly sampled in the plane $\mathcal{T}(M^i)$ tangent to the sphere at point M^i according to $\mathbf{s}^i = \cos\phi^i\mathbf{u}^i + \sin\phi^i\mathbf{v}^i$ with $\phi^i = 2\pi\xi_3^i$ where ξ_3^i is a random number $\in (0,1)$.

Due to the curvature of the space the trial move of dipole $\boldsymbol{\mu}^i$ is made in three steps in which a displacement and a rotation are involved. First, the new position $\mathbf{z}^i_{\text{new}}$ of the (randomly chosen) dipole "i" is chosen uniformly on a small cap of angle $\delta\theta$ about point M^i (i.e. the intersection of a $3D$ cone of axis $\mathbf{z}^i$ and angle $\delta\theta$ with the sphere). It is convenient to use spherical coordinates *in the local basis* $(\mathbf{z}^i, \mathbf{u}^i, \mathbf{v}^i)$ so as to define

$$\mathbf{z}^i_{\text{new}} = \sin\theta^i_{\text{new}}\cos\varphi^i_{\text{new}}\mathbf{u}^i + \sin\theta^i_{\text{new}}\sin\varphi^i_{\text{new}}\mathbf{v}^i + \cos\theta^i_{\text{new}}\mathbf{z}^i \tag{C1}$$

The choice $\cos\theta^i_{\text{new}} = (1-\cos\delta\theta)\xi_4^i + \cos\delta\theta$ and $\varphi^i_{\text{new}} = 2\pi\xi_5^i$ where ξ_4^i and ξ_5^i are random numbers $\in (0,1)$ ensures a uniform sampling of the cap. The new local basis at point $\mathbf{z}^i_{\text{new}}$ is then given by

$$\mathbf{u}^i_{\text{new}} = \cos\theta^i_{\text{new}}\cos\varphi^i_{\text{new}}\mathbf{u}^i + \cos\theta^i_{\text{new}}\sin\varphi^i_{\text{new}}\mathbf{v}^i - \sin\theta^i_{\text{new}}\mathbf{z}^i \tag{C2}$$

$$\mathbf{v}^i_{\text{new}} = -\sin\varphi^i_{\text{new}}\mathbf{u}^i + \cos\varphi^i_{\text{new}}\mathbf{v}^i\ . \tag{C3}$$

The second step consits in rotating the vector $\mathbf{s}^i$ in the tangent plane $\mathcal{T}(M_i)$ by an incremental angle $\delta\phi_i$ so that the new vector $\mathbf{s}^i_{\text{Step1}}$ reads as

$$\mathbf{s}^i_{\text{Step1}} = \cos\delta\phi_i\mathbf{s}^i + \sin\delta\phi_i\mathbf{z}^i \times \mathbf{s}^i\ , \tag{C4}$$

where the choice $\delta\phi_i = (\xi_6^i - 0.5)\delta\phi$ with ξ_6^i some random number $\in (0,1)$ ensures a uniform sampling in the interval $(-\delta\phi/2, \delta\phi/2)$.

However vector $\mathbf{s}^i_{\mathrm{Step1}}$ does not belong to the plane $\mathcal{T}(M^i_{\mathrm{new}})$ and the third and last step of the trial MC move consists in a parallel transport of $\mathbf{s}^i_{\mathrm{Step1}}$ from the point M^i to the new a priori position M^i_{new} according to Eq. (50) $\mathbf{s}^i_{\mathrm{new}} = \tau_{M^i M^i_{\mathrm{new}}} \mathbf{s}^i_{\mathrm{Step1}}$, *i.e.*

$$\mathbf{s}^i_{\mathrm{new}} = \mathbf{s}^i_{\mathrm{Step1}} - \frac{\mathbf{s}^i_{\mathrm{Step1}} \cdot \mathbf{z}^i_{\mathrm{new}}}{1 + \cos\theta^i_{\mathrm{new}}} (\mathbf{z}^i + \mathbf{z}^i_{\mathrm{new}}) \ . \tag{C5}$$

The trial displacement of dipole $\mathbf{s}^i$ is then accepted or rejected according to the standard Metropolis criterion [33] after testing the overlaps and the energies. If the trial move is accepted we make the substitutions $\mathbf{z}^i_{\mathrm{new}} \to \mathbf{z}^i$, $\mathbf{u}^i_{\mathrm{new}} \to \mathbf{u}^i$, $\mathbf{v}^i_{\mathrm{new}} \to \mathbf{v}^i$, and $\mathbf{s}^i_{\mathrm{new}} \to \mathbf{s}^i$. In the numerical experiments reported in Sec. V the parameters $\delta\theta$ and $\delta\phi$ were chosen in such a way that the acceptance ratio was ~ 0.5.

[1] J.-P. Hansen, D. Levesque, and J.-J. Weis, Phys. Rev. Lett., **43**, 979 (1979).

[2] J.-M. Caillol, D. Levesque, J.-J. Weis, and J.-P. Hansen, J. Stat., Phys., **28**, 325 (1982).

[3] J.-M. Caillol, and D. Levesque, Phys. Rev. **B 33**, 499 (1986).

[4] J.-M. Caillol, Thèse de 3ème cycle, Orsay, unpublished (1981).

[5] J.-M. Caillol, D. Levesque, and J.-J. Weis, Mol. Phys. **44**, 733 (1981).

[6] J.-M. Caillol and D. Levesque, J. Chem. Phys. **94**, 597 (1991).

[7] J.-M. Caillol and M. Trulsson, J. Chem. Phys. **141**, 124111 (2014).

[8] H. S. Cohl, Sigma **7**, 108 (2011).

[9] A. Delville, R.J.M. P7ellenq, and J.-M. Caillol, J. Chem. Phys. **106**, 7275 (1997).

[10] J.-M. Pellenq, J.-M. Caillol, and A. Delville, J. Phys. Chem. **B 101**, 8584 (1997).

[11] A. Delville, N. Gasmi, R.J.M. Pellenq, J.-M. Caillol, and H. van Damme, Langmuir **14**, 5077 (1998).

[12] M. Mazars, J.-M. Caillol, J.-J. Weis, and D. Levesque, Condensed Matter Physics, **4**, 697 (2001).

[13] J.-J. Weis, D. Levesque, and J.-M. Caillol, J. Chem. Phys. **109**, 7486 (1998).

[14] I. Shani, T. Beatus, R. H. Bar-Ziv, and T. Tlusty, Nature Physics, **10**, 140 (2014).

[15] L. Landau and E. Lifchitz, *The Classical Theory of Fields* (Pergamon,New York, 1962).

[16] J.-M. Caillol, J. Chem. Phys. **99**, 8953 (1993).

[17] R. L. Fulton, J. Chem. Phys. **68**, 3089 (1978).

[18] R. L. Fulton, J. Chem. Phys. **68**, 3095 (1978).

[19] R. L. Fulton, J. Chem. Phys. **78**, 6865 (1983).

[20] J.-M. Caillol, J. Chem. Phys. **96**, 1455 (1992).

[21] G. P. Morriss and J. W. Perram , Physica, **129A**, 395 (1985).

[22] J. W. Perram and S. W. de Leeuw, Physica, **109A**, 237 (1981).

[23] J. D. Jackson, *Classical Electrodynamics* (John Wiley & Sons, New York, 1962).

[24] C. G. Joslin and C. G. Gray, Mol. Phys. **50**, 329 (1983).

[25] K. Atkinson and W. Han, *Spherical Harmonics and Approximations on the Unit Sphere : an Introduction* (Lecture Notes in Mathematics, 2044, Springer, Berlin Heidelberg, 2012).

[26] L. Côté, M. J. Gander, L. Laayouni, and S. Loisel, *Domain Decomposition methods in Science*

and engineering (Springer, Berlin Heidelberg, 2005).

[27] J.-M. Caillol, J. Phys. Lett. **42**, L245 (1981).

[28] L. Blum and A. J. Torruella, J. Chem. Phys. **56**, 303 (1972).

[29] J.-M. Caillol, J. Chem. Phys. **96**, 7039 (1992).

[30] H. J. C. Berendsen, "Molecular Dynamics and Monte Carlo Calculations on Water", CECAM Report No 29, 1972.

[31] D. Frenkel and B. Smit, *Understanding Molecular Simulation* (Academic, New York, 1996).

[32] J.-M. Caillol, J. Chem. Phys. **98**, 9835 (1993).

[33] N. Metropolis, A. W. Rosenbluth, M. N. Rosenbluth, A. H. Teller, and E. Teller, J. Chem. Phys. **21**, 1087 (1953).

N	βu^{mono}	ϵ^{mono}	$g^{00\ \mathrm{mono}}(\sigma)$	$h^{\Delta\ \mathrm{mono}}(\sigma)$	$h^{D\ \mathrm{mono}}(\sigma)$	Z^{mono}
250	-1.78533(8)	18.14(3)	4.335(1)	2.821(2)	4.580(2)	3.954(2)
500	-1.78765(7)	18.09(3)	4.340(1)	2.819(2)	4.582(2)	3.970(2)
1000	-1.78876(8)	17.98(5)	4.341(1)	2.823(2)	4.577(2)	3.977(2)
2000	-1.78946(8)	17.93(7)	4.342(1)	2.817(2)	4.575(2)	3.981(2)
4000	-1.78969(8)	18.22(10)	4.339(1)	2.816(2)	4.571(2)	3.980(2)
∞	-1.78999(5)	-	-	-	-	-
N	βu^{bi}	ϵ^{bi}	$g^{00\ \mathrm{bi}}(\sigma)$	$h^{\Delta\ \mathrm{bi}}(\sigma)$	$h^{D\ \mathrm{bi}}(\sigma)$	Z^{bi}
250	-1.79010(7)	18.06(2)	4.334(1)	2.800(2)	4.583(2)	3.962(2)
500	-1.78998(8)	18.01(3)	4.339(1)	2.811(2)	4.579(2)	3.974(2)
1000	-1.79003(8)	17.83(5)	4.339(1)	2.814(2)	4.575(2)	3.974(2)
2000	-1.79005(8)	17.75(7)	4.338(1)	2.814(2)	4.569(2)	3.978(2)
4000	-1.79000(8)	17.96(10)	4.334(1)	2.809(2)	4.562(2)	3.975(2)
∞	-1.79000(6)	-	-	-	-	-

TABLE I: Number of particles N, reduced internal energy per particle βu, dielectric constant ϵ, contact values $g^{00}(\sigma)$, $h^{\Delta}(\sigma)$, and $h^{D}(\sigma)$ of some projections of the pair correlation function, and compressibility factor $Z = \beta P/\rho$ of the DHS fluid in the state ($\rho^* = 0.7$, $\mu^{*2} = 2$) for mono-dipoles (top) and bi-dipoles (bottom). The number in bracket corresponds to *two standard deviations* and gives the accuracy of the last digits. The thermodynamic limit of the internal energies were obtained from a linear regression in the variable N^{-1}. For each state $N_{\mathrm{Conf.}} = 16.0 \times 10^9$ configurations were generated.

N	βu^{mono}	ϵ^{mono}	$g^{00\ \mathrm{mono}}(\sigma)$	$h^{\Delta\ \mathrm{mono}}(\sigma)$	$h^{D\ \mathrm{mono}}(\sigma)$	Z^{mono}
250	-4.1625(3)	43.94(9)	5.143(2)	5.531(4)	7.146(3)	1.660(2)
500	-4.1670(3)	44.36(13)	5.142(2)	5.523(3)	7.135(3)	1.667(2)
1000	-4.1693(3)	42.99(18)	5.136(2)	5.513(4)	7.123(3)	1.665(2)
2000	-4.1703(3)	42.57(26)	5.133(2)	5.507(4)	7.117(3)	1.664(2)
4000	-4.1710(3)	41.06(36)	5.123(2)	5.495(4)	7.099(3)	1.656(2)
∞	-4.17148(16)	-	-	-	-	-
N	βu^{bi}	ϵ^{bi}	$g^{00\ \mathrm{bi}}(\sigma)$	$h^{\Delta\ \mathrm{bi}}(\sigma)$	$h^{D\ \mathrm{bi}}(\sigma)$	Z^{bi}
250	-4.1722(3)	44.55(9)	5.136(2)	5.501(3)	7.141(3)	1.657(2)
500	4.1718(3)	43.96(11)	5.136(2)	5.506(4)	7.131(3)	1.657(2)
1000	-4.1717(3)	43.24(18)	5.132(2)	5.502(4)	7.117(3)	1.662(2)
2000	-4.1714(3)	42.89(27)	5.122(2)	5.487(4)	7.103(3)	1.655(2)
4000	-4.1714(3)	45.14()	5.137(2)	5.510(4)	7.123(3)	1.670(2)
∞	-4.17138(15)	-	-	-	-	-

TABLE II: Same as Table I but for the state ($\rho^* = 0.6$, $\mu^{*2} = 4$).

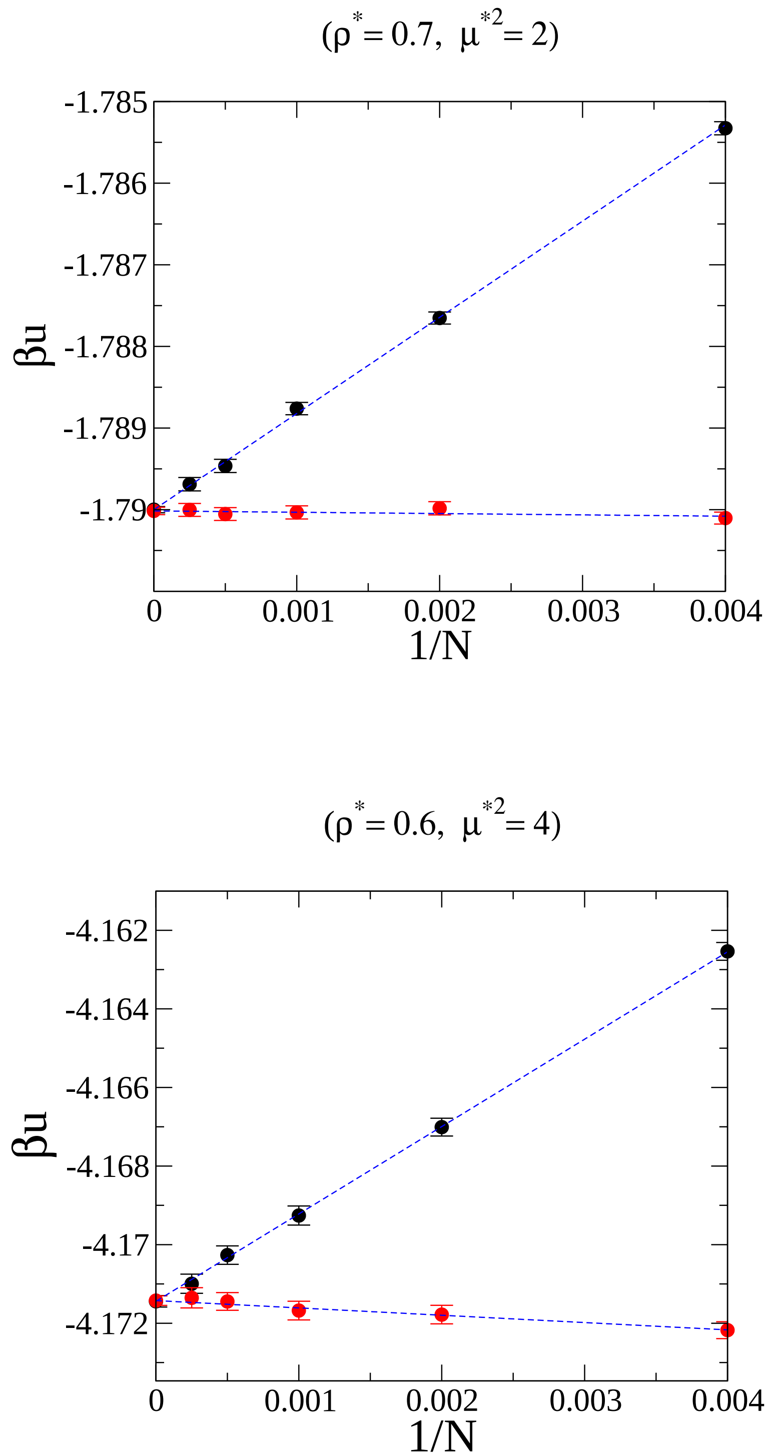

FIG. 1: Dimensionless MC internal energy βu versus the inverse number of particles $1/N$ for the states ($\rho^* = 0.7$, $\mu^{*2} = 2$) (top) and ($\rho^* = 0.6$, $\mu^{*2} = 4$) (bottom). Black circles : mono-dipoles, red circles : bi-dipoles. The error bars correspond to two standard deviations. Blue dashed lines : linear regressions.

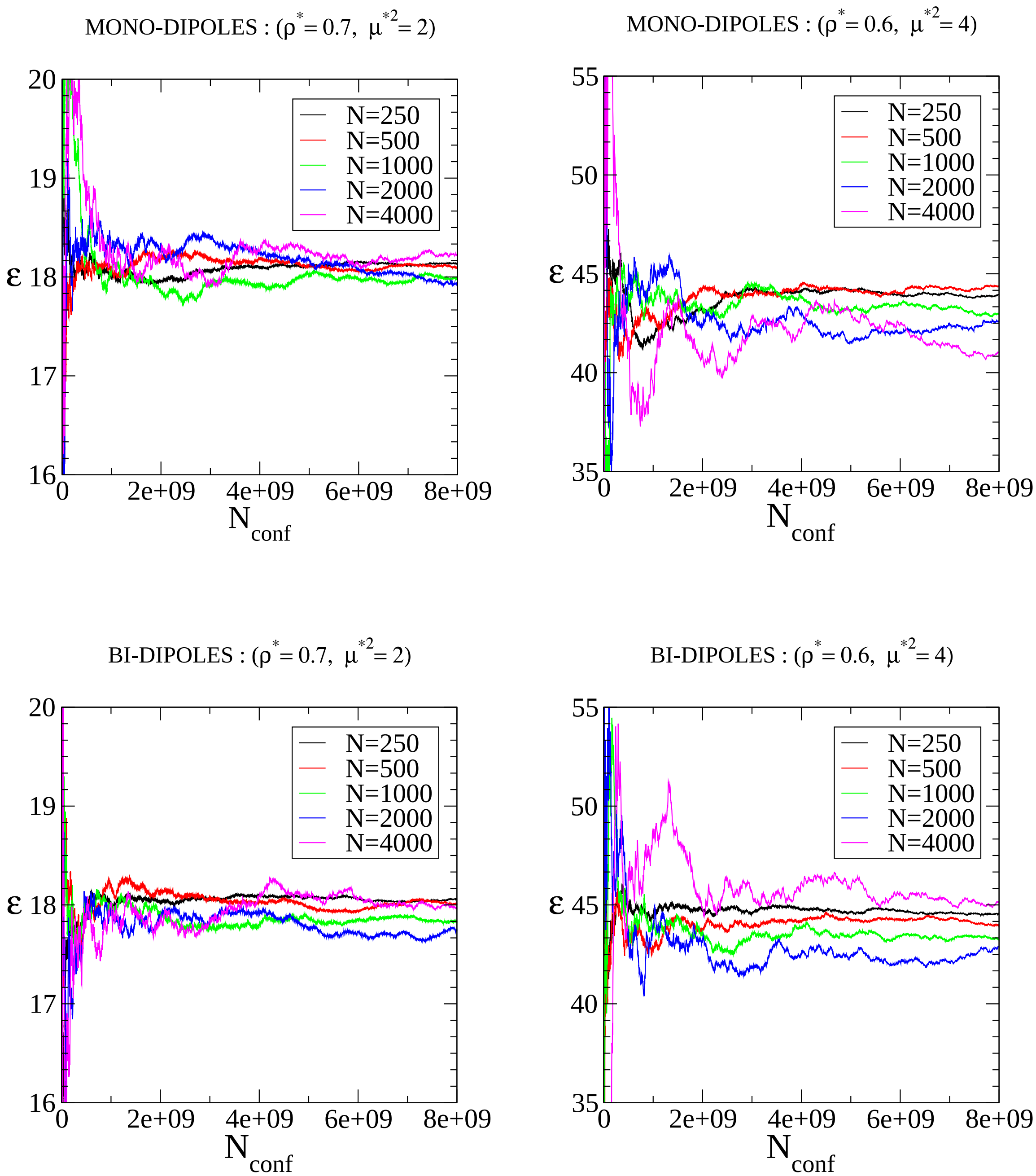

FIG. 2: Cumulated dielectric constant ϵ for the states I $\equiv$ ($\rho^* = 0.7$, $\mu^{*2} = 2$) (left) and II $\equiv$($\rho^* = 0.6$, $\mu^{*2} = 4$) (right) as a function of the number of configurations $N_{\rm conf}$. Top : mono-dipoles, bottom : bi-dipoles.

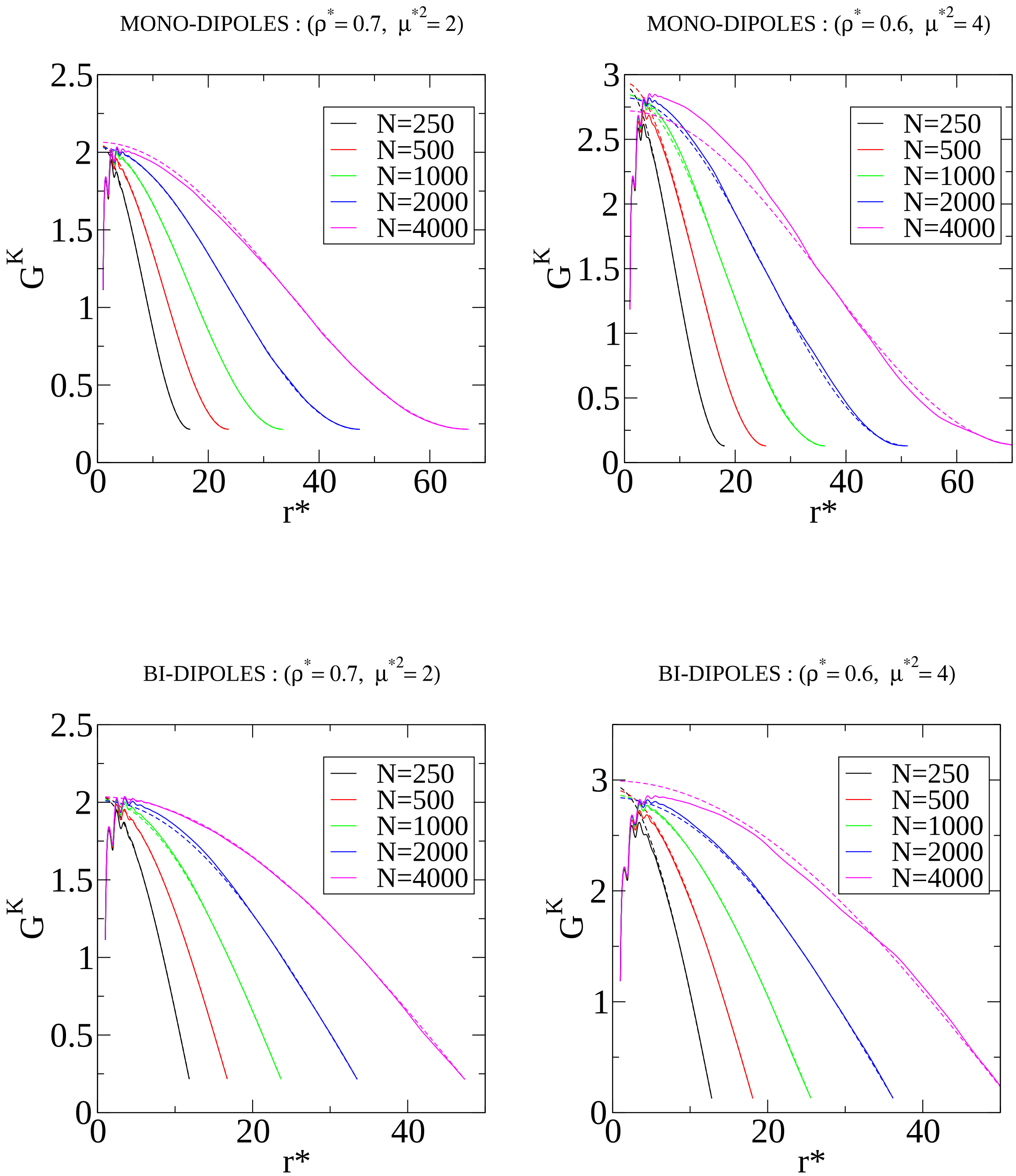

FIG. 3: Kirkwood's factor G^K for the states I$\equiv$($\rho^* = 0.7$, $\mu^{*2} = 2$) (left) and II$\equiv$($\rho^* = 0.6$, $\mu^{*2} = 4$) (right) and various numbers N of particles as a function of the reduced distance $r^* = r/\sigma$. Top : mono-dipoles, bottom : bi-dipoles. Solid lines : MC data, dashed lines : asymptotic behaviors given by Eq. (78) for mono-dipoles and Eq. (88) for bi-dipoles.

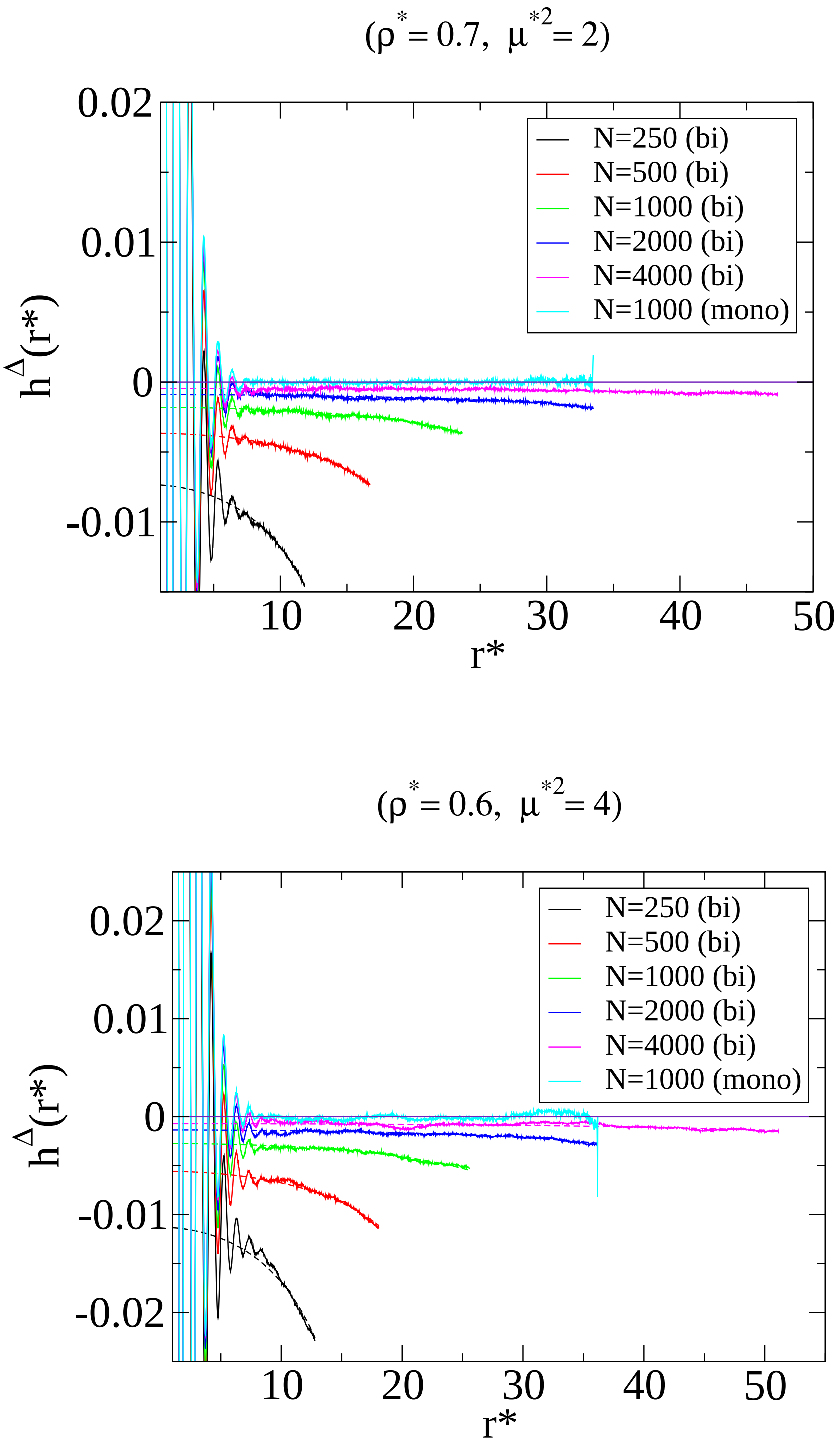

FIG. 4: Projection $h^{\Delta}(r^*)$ for the states I$\equiv(\rho^* = 0.7,\ \mu^{*2} = 2)$ (top) and II$\equiv(\rho^* = 0.6,\ \mu^{*2} = 4)$ (bottom) and various numbers N of particles (bi-dipoles) and $N = 1000$ (mono-dipoles). Solid lines : MC data, dashed lines : asymptotic behavior.

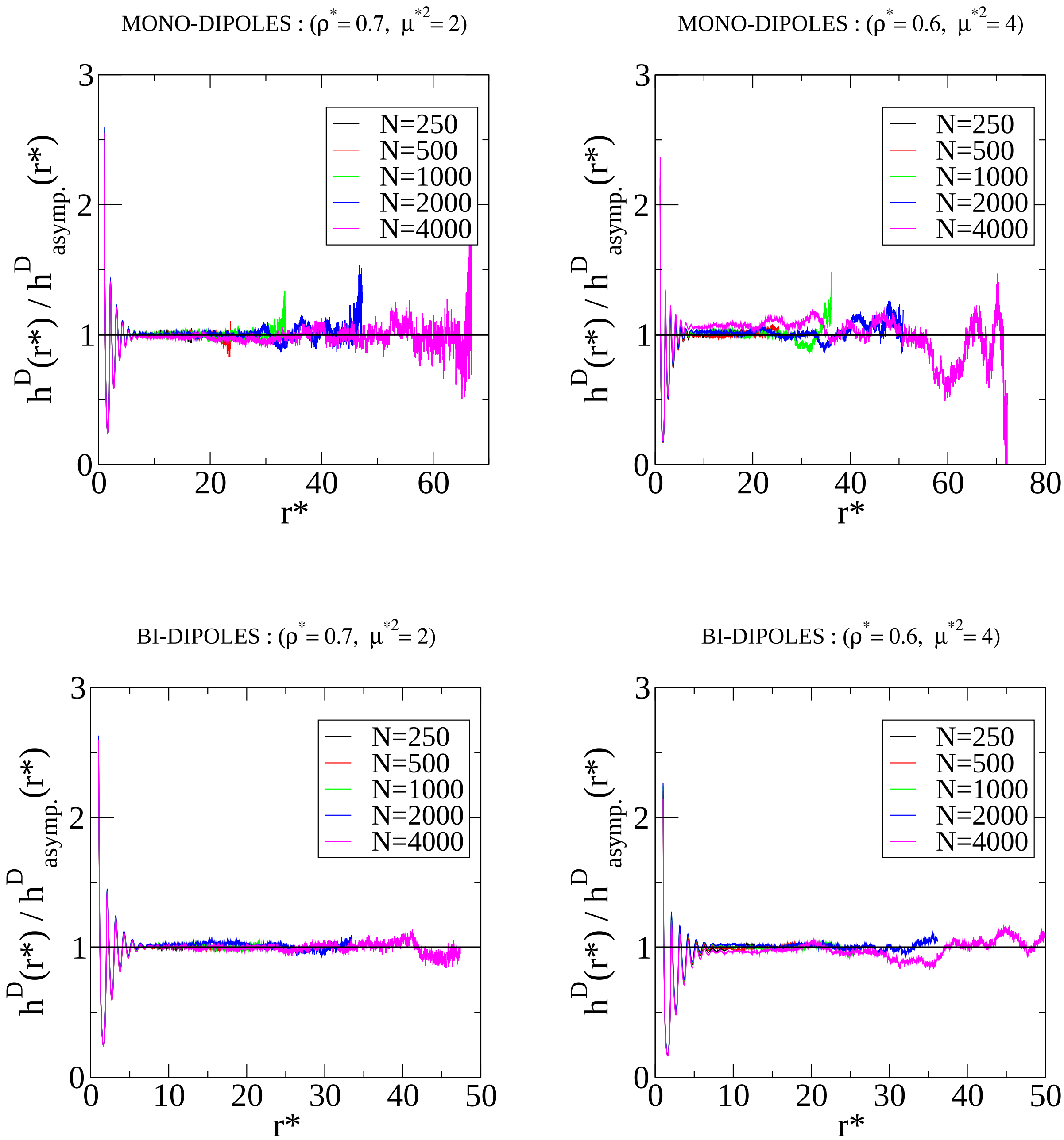

FIG. 5: Ratio $h^D(r^*)/h^D_{\text{asymp.}}(r^*)$ for the state I≡($\rho^* = 0.7$, $\mu^{*2} = 2$) (left) and II≡($\rho^* = 0.6$, $\mu^{*2} = 4$) (right) and various numbers N of particles. Top : mono-dipoles, bottom : bi-dipoles.